Manuel Zettl, BSc

Investigation of a Continuous Tablet Coater

via Optical Coherence Tomography

MASTERARBEIT

zur Erlangung des akademischen Grades

Diplom-Ingenieur

Masterstudium Verfahrenstechnik

Eingereicht an der

Technischen Universität Graz

Betreuer

Univ.-Prof. Dipl.-Ing. Dr.techn. Johannes Khinast

Institut für Prozess- und Partikeltechnik

Dr.techn. Dipl.-Ing. Patrick Wahl, BSc

Research Center Pharmaceutical Engineering GmbH

STATUTORY DECLARATION

I declare that I have authored this thesis independently, that I have not used other than the declared sources / resources, and that I have explicitly marked all material which has been quoted either literally or by content from the used sources. The uploaded file on TUGRAZonline is identical with this version of the thesis.

…………………..   …………………………………..

date   (signature)

EIDESSTATTLICHE ERKLÄRUNG

Ich erkläre an Eides statt, dass ich die vorliegende Arbeit selbstständig verfasst, andere als die angegebenen Quellen/Hilfsmittel nicht benutzt, und die den benutzten Quellen wörtlich und inhaltlich entnommene Stellen als solche kenntlich gemacht habe. Das in TUGRAZonline hochgeladene Textdokument ist mit der vorliegenden Masterarbeit identisch.

Graz, am …………………….   …………………………………..

(Unterschrift)

Acknowledgments

Kurzfassung

Bisher sind diskontinuierliche Prozesse, auch Batch Prozesse genannt, der Stand der Technik in der Pharmaindustrie. Um Energie und Zeit zu sparen gibt es vermehrt Bestrebungen die bestehenden Prozesse durch kontinuierliche zu ersetzen, bei gleichbleibender oder steigender Produktqualität. In dieser Arbeit wird die Analyse von Coating-Schichtdicken, die in einem semi-kontinuierlichem Tablettencoater (DRIACONTI-T pharm Lab) erzeugt werden, mithilfe von optischer Kohärenztomographie (OCT) ausgewertet. In diesem Coater gibt es drei Kammern, jeweils mit einer Füllmenge von 1.8l Tablettenvolumen. Dadurch können die Tabletten schrittweise durch den Beschichtungsprozess geführt werden. Um optimale Betriebspunkte des Beschichtungsprozesses zu finden, wird eine statistische Versuchsplanung (DoE) in der dritten Kammer durchgeführt, bei der die Temperatur der eingelassenen Luft, die Sprührate und der Zerstäubungsdruck der Düsen variiert werden und der Sprühdruck, die Trommeldrehzahl und die Tablettenmasse konstant bleiben. Dabei werden beim Prozess die Ablasstemperatur der Luft aufgezeichnet und die gesamte aufgesprühte Coatingmasse und der daraus resultierende Sprühverlust bestimmt. Eine Stichprobe von 10 Tabletten pro Versuch wird hinsichtlich Gewichtszunahme, Durchmesserzunahme und Schichtdicke untersucht. Die Coatingmasse und Schichtdicke der Versuche wird mit einem mathematischen Modell verglichen, bevor die Resultate in MODDE 11 evaluiert werden und der Einfluss der verschiedenen Prozessparameter diskutiert wird. Außerdem wird ein semikontinuierlicher Prozess geprüft, bei dem Augenmerk sowohl auf die Temperaturverläufe der einzelnen Kammern, als auch auf Coatingmasse und Schichtdicke der einzelnen Batches gelegt wird. Um die Durchführbarkeit von OCT-Messungen bei gefärbten Tabletten zu evaluieren, werden Versuche mit einem wasserlöslichen (Indigocarmin) und einem festen (Eisen-III-Oxid) Farbstoff durchgeführt und die Qualität der erhaltenen Daten wird analysiert.

Abstract

Until now discontinuous processes, so-called batch processes, are the state of the art of the pharmaceutical industry. To save energy and time, there are increasing efforts to replace the existing process with continuous ones, with equal or improved product quality. This thesis deals with the analysis of the coating thickness on tablets, which were produced in a semi-continuous tablet coater (DRIACONTI-T pharm Lab) via the means optical coherence tomography (OCT). This coater has three chambers, each with a tablet filling volume of 1.8l. Therefore, the tablets can be guided through the process step-by-step. In order to find optimal parameters for the coating process, a design of experiments (DoE) is executed in the third chamber, where the inlet air temperature, the spraying rate and the pattern pressure of the nozzle are varied and the atomizing air pressure of the nozzle, the drum rpm and the tablet mass are kept constant. At the process the exhaust air temperature and the total coating mass, with the resulting spray loss, are measured. A sample of 10 tablets per trial is analyzed concerning weight gain, diameter gain and coating thickness. The coating mass and coating thickness of the trials is compared to a mathematical model, before the results are evaluated in MODDE 11 and the parameter influence is discussed. Additionally, a semi-continuous run is examined, looking at the temperature profiles in the chambers, as well as the coating mass and coating thickness of the different batches. To evaluate the practicability of OCT-measurements concerning colorants, trials with a water-soluble (indigo carmine) and a solid (iron-III-oxide) dye are executed and the quality of the obtained data is analyzed.

Abbreviations

A	Surface Area of biconvex tablets
AC	Air Conditioning
API	Active Pharmaceutical Ingredient
CAP	Celluloseacetatephtalate
D	Tablet Diameter
DoE	Design of Experiments
E	Tablet Porosity
E_Y	Young's Modulus of Elasticity
EC_{aq}	Aqueous Ethylcellulose
F	Compression Force
FDA	US Food and Drug Administration
Fe_2O_3	Iron-III-Oxide
GMP	Good Manufacturing Practice
h	Characteristic length for biconvex tablets
H	Characteristic length for biconvex tablets
H_C	Thickness at the point of compression
HPMC	Hydroxypropylmethylcellulose
HPMCP	Hydroxypropylmethylcellulosephthalate
K_r	Porosity of the powder bed where the pressure is zero
K_y	Material dependent constant inversely proportional to yield pressure
MCC	Microcrystalline cellulose
MFT	Minimum film forming temperature
OCT	Optical coherence tomography
P_C	Compression pressure, for a flat round tablet
P	Tablet hardness
PAMA	Polyacrylmethacrylate
r	Radius of a biconvex tablet
s	Thickness of a biconvex tablet
SDOCT	Spectral Domain Optical Coherence Tomography
SNR	Signal to Noise Ratio
t	Tablet thickness
TDOCT	Time Domain Optical Coherence Tomography
T_g	Glass transition temperature
V	Volume of biconvex tablets

w	Tablet weight
WHO	World Health Organization
WR	Characteristic length of a biconvex tablet
ε	Deformation strain
ρ$_t$	True density of the tableting mass
σ	Tablet tensile strength
σ$_d$	Deformation stress

List of Figures

List of Tables

List of Equations

Index

1. Introduction and Aim of the Thesis

The pharmaceutical industry has shown a strong tendency to implement continuous processes, after the US Food and Drug Association (FDA) published new guidelines for good manufacturing practice (GMP) in 2004 [1]. Especially tablet coating processes have been performed batch-wise for a long period of time, therefore continuous implementations are relatively new [2]. The need for non-destructive in-line analysis methods for such processes is imminent [3].

The motivation of this thesis is to evaluate a DRIAM DRIACONTI-T tablet coater, with the aid of optical coherence tomography (OCT). Therefore, a design of experiments (DoE) is created and run, to achieve a profound process understanding and to find optimal coating conditions. For the DoE, 11 experiments are performed where the factors flow rate, inlet air temperature and pattern pressure of the nozzle are varied, while the atomizing air pressure of the nozzle, tablet mass and drum rpm are kept constant. The obtained data is investigated in MODDE 11 concerning the responses flow rate, inlet and outlet temperature, coating thickness, inter- and intra-variability of the coating, pattern pressure as well as spray loss and coating mass. Also a semi-continuous run is executed, to evaluate the possibility of a continuous coating run in this equipment. Furthermore, colorant trials are analyzed to see if they can be measured meaningfully by the means of OCT.

In Chapter 2, a literature research on the topics of OCT, tablets and tableting, coatings and coaters is committed. Chapter 3.1 and Chapter 3.2 deal with the used materials and methods and a detailed description of all performed experiments, finalized with possible process ameliorations. Subchapter 3.3 describes the data evaluation of the DoE, and a comparison between a mathematical coating growth model. It also states possible meaningful process parameters. The thesis is ended with a conclusion and an outlook for the future in Chapter 4.

2. Theoretical Background

This chapter introduces the theory behind the performed experiments and process evaluation. Therefore, an overview over tablets and tableting, optical coherence tomography (OCT) and coating, with focus on tablet coating, will be given.

2.1. Tablets and Tableting

In this subchapter, which is based on [4], the principles of tablets and the tableting process are explained. The focus lies on the physical and chemical properties of the tablets and their components, as well as the tablet manufacturing itself.

2.1.1. Ingredients

A tablet is usually made of the active pharmaceutical ingredient (API) and at least one other excipient. Other excipients include disintegrants, glidants, lubricants and antiadherents, and are chosen to ameliorate the properties of the final tablet [5].

Concerning the API, being the biologically active substance in the organism, it is essential to have a high uniformity throughout the tablets. This is to ensure the same amount of API per tablet and constant release characteristics [5].

Disintegrants are added to break up the tablet in aqueous media such as the mouth or the stomach, depending on the location of drug release. The two main groups of disintegrants are the traditional ones, and so-called superdisintegrants. Until the late 1960s, where the first superdisintegrants were discovered, the traditional disintegrants were used and some are still used today, such as native starches, alginic acid and ion-exchange resins. However, modern superdisintegrants show a much higher effectivity at already low concentrations. Main examples are sodium starch glycolate, croscarmellose sodium or crospovidone. Some of these materials can show cross-reactions with the API. If this is the case, there are other alternatives, such as microcrystalline cellulose (MCC), low substituted hydroxypropyl cellulose, soy polysachharide, xylan, xanthan SM and inorganic materials like aluminum silicates [5].

There are three groups of lubricants, that promote different purposes. The first objective is to support particle flow to create a homogenous die fill, resulting in a uniform tablet weight. This group is called glidants. The function of the second group, anti-adherents, is to suppress the adhesion to the tablet punch during the ejection from the die. The third groups purpose

is to overcome the sticking to the sides of the tablet in the die. This group is usually referred to as lubricants. There are many materials that show one or more of these behaviors. Typical lubricants and antiadherents are metallic salts of fatty acids, esters of fatty acids, fatty acids, alcohols, oils, acids and other materials such as starch and talcum. The most commonly used glidants are calcium silicate, cellulose, colloidal silicon dioxide, magnesium oxide, magnesium silicate, starch and talcum [5].

2.1.2. Mixture Preparation

Once the tablet composition is found, a way to prepare a perfect mixture is necessary. As the blend uniformity is influenced by a magnitude of factors, like the particle shape, size, density and cohesivity and additionally by the parameters of the blending process itself [6].

As segregation is a main issue after the mixing process, it usually is advantageous to mix ingredients with similar particle sizes. To generate this homogeneity, the particles are either milled or granulated prior to the blending step or chosen in the right size from the beginning. While cubic and spherical particles show better flowing properties than needle and plate shaped ones, and are therefore mixed more easily, they tend to segregate after the mixing process more readily. Another impact for segregation can be density differences, but often only in combination with particle size inhomogeneity or enormous density differences, where one density is four times the other [6].

To ensure a high uniformity it is vital to eliminate cohesion as thoroughly as possible, as agglomerates would destroy a tablets homogeneity. The causes of cohesion include several forces, mainly electrostatic, mechanical, surface tension and Van der Waals forces. In combination, these effects are bigger than the particle weight and their amount depends on size, shape, morphology, moisture and packing density of the handled substances. To achieve a uniform powder, often an external stress has to be applied on cohesive materials, therefore they are often milled before mixing and handled with great care afterwards [6].

The mixing process unites three different mechanisms, being diffusion, convection and shear. In diffusive mixing, random particle movement based on the concentration differences of the substances leads to a randomization. This is often referred to as micro-mixing. Macro-mixing, more commonly known as convection, is the movement of neighboring particles within a powder bed. Finally shear mixing is created by applying a mechanical force on the compounds, creating slip planes or shearing strains [6].

The discontinuous blending process consists of four steps, namely the expansion of the powder bed, the activation of three-dimensional shear forces, an adequate length of time to ensure high randomization and the maintaining of this state after the process is stopped. There are several factors that affect these contributors. Chosen examples are the filling degree of the blender, which influences the residence time, and exceeding the ideal mixture time as well as altering the operating parameters, such as rotation speed, of the blender, which can negatively affect the uniformity of the blend [6].

While some materials are suitable for direct compaction, which means that the tableting process is started right after mixing of the components without further preparation being necessary, others need more elaborate preparation. These preparation possibilities include dry granulation, where the mixture is roughly compressed, wet granulation with a drying step or hot melt extrusion. These steps can be necessary to fill the die with a limited inner surface [7].

2.1.3. Parameters of the Tableting Process

To understand the different parameters that influence the formation of a tablet, one needs to understand the process first. Powder is filled, gravitationally or by suction, into a die. Afterwards force is applied onto the powder via a punch, reducing the volume and creating a solid body. Each pair of punch and die is referred to as a station. Tablet presses can be distinguished by the number of stations they have. There are either single-station presses, or industrially used multi-station rotary presses. These rotary presses can be operated from 1 to 200rpm, using 16 to 75 stations. The stations are fixed on a turret which is moved through the different compaction stages, namely the filling of the die, the adjustment of the fill weight, the tablet compaction and the tablet ejection. A compact tablet is created by rearranging the particles, as well as elastic, viscoelastic and plastic deformation and fragmentation of particles, as well as the formation of interparticle bonds, including mechanical interlocking, solid bridges and interparticle attraction forces [5].

Unwanted behavior after the compaction, include capping or tablet breakage. To minimize this behavior, the process parameters must be chosen thoughtfully. The parameters that have shown to have most influence are the compaction force, the tableting speed and the turret speed, which determines the speed of the die filling and thus the filling height and weight [5].

2.1.4. Tablet Properties

According to the International Pharmacopoeia released by the World Health Organization (WHO) [8] tablets have to be validated visually, by uniformity of mass, uniformity of content and dissolution/disintegration. For the visual test, at least 20 tablets are inspected concerning smoothness, damages and uniform color. The recommended procedure for the control of the uniformity is to weigh 20 tablets and analyze them concerning their deviation to the average mass. The limits are shown in Table 1.

Table 1: Recommended limits for the uniformity of mass according to [8].

Average mass of tablet	Deviation	Number of tablets
[mg]	[%]	[-]
Below 80	±10.0	Minimum 18
	±20.0	Maximum 2
From 80 to 250	±7.5	Minimum 18
	±15.0	Maximum 2
More than 250	±5.0	Minimum 18
	±10.0	Maximum 2

The uniformity of mass testing only applies to formulations with a quantity of 5mg or less or 5% or less of API in the formulation. The best practice, according to the WHO is to determine the API amount in each of 10 tablets. If each unit contains within ±15% of the average amount the test is passed. If there is a single tablet over the ±15% range, but does not exceed ±25% another 20 tablets of the original sample are analyzed. If these 20 tablets are in the ±15% range the test is still completed.

For the disintegration test the tablets are placed in six basket tubes, in an apparatus that is described in detail in [8]. Water, unless specified otherwise, at 35-39°C is added. At the end of the specified time all of the tablets have to be completely disintegrated. If one or two tablets fail this test, another 12 tablets are investigating. The test is passed when at least 16 out of 18 tablets disintegrate completely.

The dissolution test is performed with a meaningful dissolution medium in an apparatus that is explained in [8]. The exact procedure is as follows: "*Place the stated volume of the dissolution medium (± 1%) in the vessel of the specified apparatus. Assemble the apparatus, equilibrate the dissolution medium to 37 ± 0.5 °C, and remove the thermometer. The test*

may also be carried out with the thermometer in place, provided it is shown that results equivalent to those obtained without the thermometer are obtained. Place one dosage unit in the apparatus, taking care to exclude air bubbles from the surface of the dosage unit. Operate the apparatus at the specified rate. Within the time interval specified, or at each of the times stated, withdraw a sample from a zone midway between the surface of the dissolution medium and the top of the rotating basket or blade, not less than 1 cm from the vessel wall. Where multiple sampling times are specified replace the samples withdrawn for analysis with equal volumes of fresh dissolution medium at 37 °C or, where it can be shown that replacement of the medium is not necessary, correct for the volume change in the calculation. Keep the vessel covered for the duration of the test and verify the temperature (37 ± 0.5 °C) of the medium at suitable times. Perform the analysis as directed in the individual monograph using a suitable assay method. Test samples are filtered immediately upon sampling using in-line filtration, unless filtration is demonstrated to be unnecessary. Use an inert filter that does not cause adsorption of the active substance or contain extractable substances that would interfere with the analysis. Centrifugation is not recommended unless validated for the specific test. The test is to be conducted with six dosage form units in parallel."

There are several other criteria to test the tablets after their production, e.g. the tablet friability and hardness. Friability is tested by dusting and weighing the tablets, putting them in a rotating drum for 100 rotations and dusting and weighing them again. The number of tablets for this test is determined by the average mass of a single tablet. Tablet Hardness is measured by applying and measuring the radial force that is needed to break a tablet. The drawback of this method is that it does not provide information about the reason for failure, but on the other hand it is reproducible. Dissolution tests can be performed at different pH-Values, determined by the intended function of the tablet [2,7,9]. Meaningful values and residence times are shown in Table 2.

Table 2: pH-ranges and residence times in the body [2].

Location	pH-Range	Residence time
Mouth, Esophagus	6.4	~10s
Stomach	1 – 3.5	0.5 - 3h
Small Intestine	6.5 – 7.8	6 – 8h
Large Intestine	7.5 – 8.0	~10h

Theoretical Background

Other mechanical properties of tablets include tensile strength, indentation hardness, Young's modulus and the yield stress, that is obtained from Heckel plots. The tensile strength can be computed using the tablet hardness, diameter and thickness as shown in the following formula,

$$\sigma = \frac{2 * P}{\pi * D * t} \tag{1}$$

where σ = tablet tensile strength, P = tablet hardness, D = tablet diameter and t= tablet thickness.

Indentation hardness is a measure of the local plasticity of a material. Therefore, an indenter or pendulum is used from a known distance to the surface of the tablet. To calculate the resistance to indentation of the tablet one can divide the energy of impact by the volume of indentation. As a measure for the stiffness and toughness of a material, the Young's modulus was introduced. It is defined as

$$E_Y = \frac{\sigma_d}{\varepsilon} \tag{2}$$

where E = Young's modulus of elasticity, σ_d = deformation stress and ε = deformation strain, and is usually measured by flexure testing. In order to show force-volume correlations one can use Heckel plots, as shown in Figure 1. Thus, the Heckel equation

$$-\log E = K_y * P + K_r \tag{3}$$

where:

E = porosity of the tablet,

$$E = 100 * \left[1 - \frac{4w}{\rho_t * \pi * D^2 * H_C}\right] \tag{4}$$

(w = tablet weight, ρ_t = true density of the tableting mass, H_C = thickness at the point of compression)

P_C = compression pressure, for a flat, round tablet

$$P_C = \frac{4F}{\pi \cdot D^2} \tag{5}$$

(F = compression force, D = Tablet diameter)

K_y = a material-dependent constant inversely proportional to its yield pressure and K_r = porosity of the powder bed where the pressure is zero, can be used to show this correlation [10].
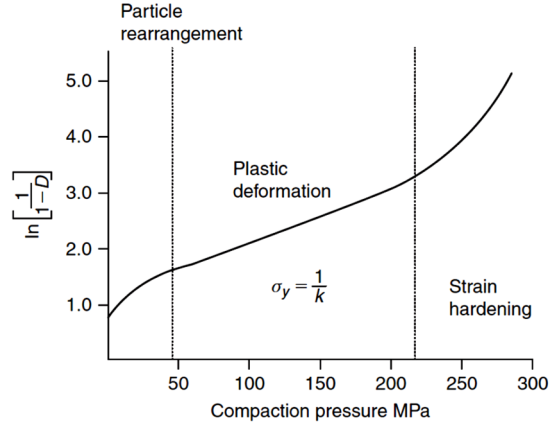
Figure 1: Heckel plot [10]

2.2. Optical Coherence Tomography

Optical coherence tomography (OCT) is a high-resolution imaging technique, mainly used in the biomedical sector, due to its contactless and non-destructive behavior. It can be used to evaluate the structure and thickness of different turbid and semi-transparent materials, by producing an in-depth profile [11]. In addition to its medical use, mainly in ophthalmology [12], it has started to attract interest in other fields, like silicon integrated circuits [13], fiber composites [14], pharmaceutical tablets and coatings [11, 15–18], as well as paper quality control [19, 20].

2.2.1. Measurement Principle

The two mainly used methods for gathering information are time-domain OCT (TDOCT) and spectral-domain OCT (SDOCT). The older existing TDOCT works as illustrated in Figure 2. The light source emits a beam, which is split into a reference and probing beam. The reference beam is directed towards a mirror and reflected, while the backscattered information from the sampling beam is also recorded. The so created interference pattern of the light waves can then be used to calculate depth profiles of the observed material. As the emitted light usually has a broad variety of wavelengths, the best interference is created when both beams have travelled the same optical length before being processed. Therefore, it is necessary that the reference path distance is adjusted to be able to obtain the depth characteristics of a sample [11].
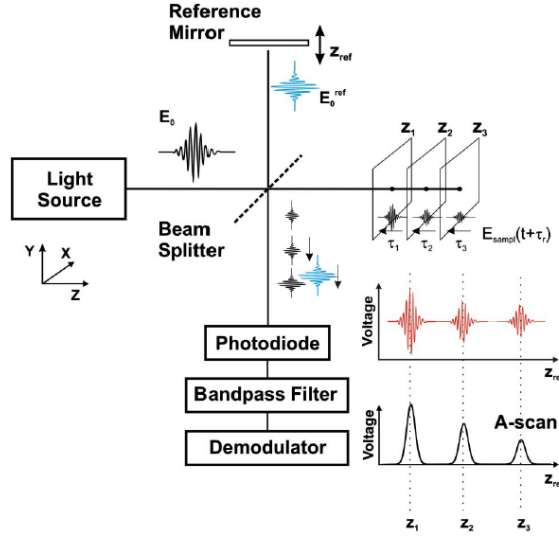
Figure 2: Schematic of a TDOCT System [22].

The ameliorated version depicted in *Figure* 3 shows a SDOCT system. The main difference to the TDOCT is that the travelling distance of the light beam in the reference path is fixed. The obtained interference pattern is analyzed with a spectrometer and Fourier transformed to get a depth profile. The SDOCT system is significantly superior to TDOCT when regarding the imaging speed and the signal to noise ratio SNR, as all echoed light is measured simultaneously [11].
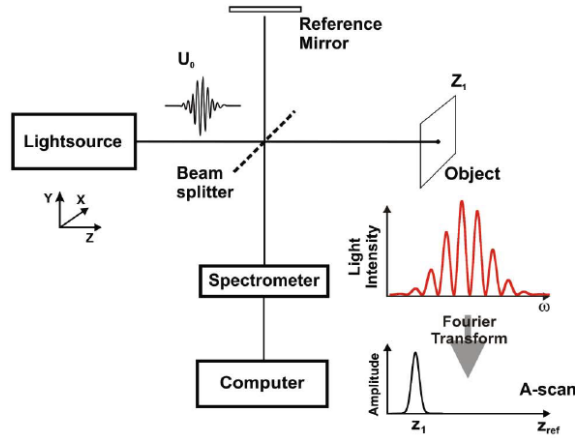
Figure 3: Schematic of a SDOCT System [22]

The used light beam is usually a low coherent infrared beam. Each single measurement creates an axial depth profile, a so-called A-scan. By either moving the sample or deflecting the light beam transversally with a mirror a 2D-profile can be created (B-scan). By deflecting the beam with two mirrors a 3D-image (C-scan) can be obtained. Concerning the resolution of the OCT system, one has to differentiate between the axial and the transversal resolution.

While the axial resolution depends on the wavelength and the bandwidth of the light source, the transversal resolution is determined by the optical lens in use [10–12, 18, 22].

2.3. Coating

Coatings have a great field of applications within the design of drugs. They can be used for a better product identification by adding dyes (e.g.), taste masking for drugs with an unpleasant taste, stability in certain pH-milieus and controlled drug release. In this subchapter the focus mainly lies on the coating of pharmaceutical tablets, including the state-of the art methods, mathematical and theoretical background and the measurement methods used to evaluate the quality of coatings [2].

2.3.1. Formulations

The used coating greatly depends on the intended purpose and the used method. The two main methods are sugar-coating and film-coating. Sugar coatings are mainly applied in pan coaters, drum coaters and fluidized beds and are used for thicker coatings and to hide surface defects. Film coatings are mainly brought onto the tablet cores in drum coaters and fluidized beds, are thinner and conserve the form of the tablet. The important process parameters for both coating processes are the spraying pressure, the temperature, the number of tablet cores and the spraying rate [2]. The focus within this thesis is on film coatings.

It can be generally spoken that the application of film coatings is less time and energy consuming than that of sugar coating. The main advantages are a reduced process time by about 66%, with a dramatically reduced energy consumption, a small weight gain of 2-3% compared to 30-50% in sugar coating, the conservation of imprints for product identification, easier process automation, easier creation of specific and uniform release and a large selection of polymers. For the coating of tablets, it is usually of advantage to use bi-convex tablets with small curvature instead of flat ones, to avoid twin-formation and abrasion [2].

For the film formation, the polymer dispersion is brought onto the tablets, while evaporating the solvent (usually water). Due to several influences, such as capillary forces and particle-solvent and particle-air interactions, the particles move closer together and finally form a continuous film [2].

The selection of a suitable polymer is based on the desired duration of the API release as well as the intended location. Fast release tablets are coated with polymers that are soluble

within a pH-range of 1-3.5 and are dissolved in the stomach. Sustained release drugs or API's that are sensitive to the very acidic milieu in the stomach are usually coated with polymers that dissolve or swell in a pH-range of 6.5-8. For sustained release the API diffuses through the swollen coating.

There are several properties the used materials should have, to be optimally suiTable for coating purposes. First of all, they have to be soluble or dispersible in the desired solvent, which is usually water. Second, their solubility behavior should meet the coating purpose, regarding the dissolving time and pH-range. Additionally, they should be able to form a smooth, nice surface, be resistant to heat, light, humidity, air and the coated substrate, show no ageing under a defined environment, have neither odor, taste or color, be harmless to the human health, have compatibility to the API's and excipients in the tablet, as well as the common film excipients, such as plasticizers, colorants and tacking agents. Last but not least they should be stable without cracking due to mechanical forces, build a barrier against environmental influences for the tablet, and don't fill up possible imprints. As no known polymer has all of these characteristics, they are usually selected according to the three main criteria, solubility or dispersion behavior in the solvent, location and duration of the API release and the film forming capability, and are then combined with other ingredients [2].

Enteric coatings, i.e. coatings that are resistant to gastric juices, were long made out of celluloseacetatephtalate (CAP) but were replaced by polyacrylmethacrylates (PAMA) due to the advantage of being able to use water as a solvent. In Japan also hydroxypropylmethylcellulosephthalate (HPMCP) is used to a large extent. All of these materials can also be combined with colorants [2].

Similar to enteric coatings, films with sustained release characteristics were usually created with polymers in organic solvents. Nowadays, the two most used materials are PAMA- and aqueous ethylcellulose (EC_{aq}). As sustained release films are very complex systems, they are usually not colored themselves. If a color is desired, the tablets are usually coated with an additional, fast release coating with the desired color [2].

Aesthetic, or fast release, coatings are usually polymers that are readily soluble within water. Within this group hydroxypropylmethylcellulose (HPMC) is by far the most important one, accounting to about 60-70%, or about 10000 tons of this group per year [2].

2.3.2. Drum Coaters

In a drum coater, the tablets are coated in a rotating, cylindrical drum. The tablets are mixed by the rotation and the coating suspension is sprayed onto the tablets via one or more nozzles. At the same time the coating is dried via a temperature-controlled inlet air-stream. To increase the mixing inside the drum, barriers can be added. However, care has to be taken that no dead-zones arise due to these modifications [2].

The quality of the coating depends on numerous factors. First of all, one has to make sure that there is the right amount of tablets (i.e. not too less or too many) inside the drum, so that they can mix and move properly. This amount is given by the tablet geometry and density. Also it has to be kept in mind that for high rotational speeds of the drum, abrasion of the tablets can occur [2].

Another aspect that can explain varying coating results is the relative humidity of the air-stream, as the drying capacity shrinks with increasing humidity. For controlling these fluctuations, an air-conditioning can be installed prior to the process [2].

Additionally, the atomizing pressure has a huge impact on the distribution of the suspension droplets and therefore on the coating uniformity. The higher the atomizing pressure is, the smaller are the droplets that are created, increasing the available surface area for solvent evaporation. This can lead to a drying of the droplets before they hit the tablets, influencing the spray loss and the coating growth. The number and distance of nozzles has to be carefully thought of, as overlapping spraying areas can lead to an environment, where the tablets get too wet and tend to stick to each other or to the wall. This effect can also be observed at high flowrates, making an optimization of spraying rate and pressure complicated [2].

2.3.3. Problems

There are several problems that can occur during or after a coating process. First of all, orange skin can appear, as well as peeling, flaking, spalling, pimple formation, twin formation, broken coatings, porous coatings, fibrous coatings, scuffing and capping. All of these problems can be eradicated by altering the process conditions [2].

2.3.4. Characterization

To evaluate and characterize coatings a multitude of different methods is available, for both, films only and coated materials. Examined properties include homogeneity, solubility, mechanical properties, wetting properties, permeability, surface properties, thickness and thermal properties [2].

The homogeneity of the coated tablets is evaluated by weighing them after the process, and comparing each tablet to the mean mass. The allowed deviation depends on the mean mass, and is 10% for tablets weighing 80mg or less, 7.5% for the range between 80 and 250mg and 5% for a weight of 250mg or above [2].

Thermal characteristics that are important are the minimum film forming temperature MFT and the glass transition temperature T_g. The MFT is defined as the temperature, above which a polymer dispersion forms a film without cracks under defined parameters. Above T_g amorphous polymers show a liquid or elastic state [2].

The solubility of the coating is important for the location and duration of the API release. Fast release drugs are coated with substances that are soluble in the pH range of 1-3.5, so that they are released within the stomach. For sustained release or enteric coatings, a solubility in the 6.5-8 range is needed, to ensure a diffusion of the API in the gastro-intestinal tract. For the examination of the solubility behavior at least 3 dissolution tests are performed [2].

For the characterization of the coating thickness several possibilities exist. Terahertz imaging (THI) also is a direct measurement method, which is capable of penetrating layers of strongly scattering materials, but with lower resolution [18]. Raman [24], and near-infrared (NIR)-spectroscopy [25] are non-destructive as well, however have the drawback to OCT, that they need a profound calibration and good models. Also microscopy [26] and measuring the diameter gain of the tablets can be used, but are very time-consuming when compared to OCT, as an automated process has to be established to analyze the tablets.

3. Practical Exercise

In this chapter the practical work is explained. First the used equipment and materials are described, followed by the conducted experiments and obtained results. Afterwards, the data is evaluated and analyzed. Finally, the arisen problems are discussed.

3.1. Experimental Setup

3.1.1. Equipment

The OCT-system in use is OSeeT Pharma 1D, produced by Phyllon GmbH in Graz. It has an axial resolution of 4µm and a transversal resolution of 14µm, while having an A-scan rate of 60kHz, corresponding to about 60 images per second.

The trials are performed in a DRIACONTI-T® pharma LAB coater, a mini-batch tablet coater suitable for continuous coating purposes. It consists out of three chambers, with a filling volume of 1.8l of tablets each, that can be seen in Figure 4 and Figure 5.
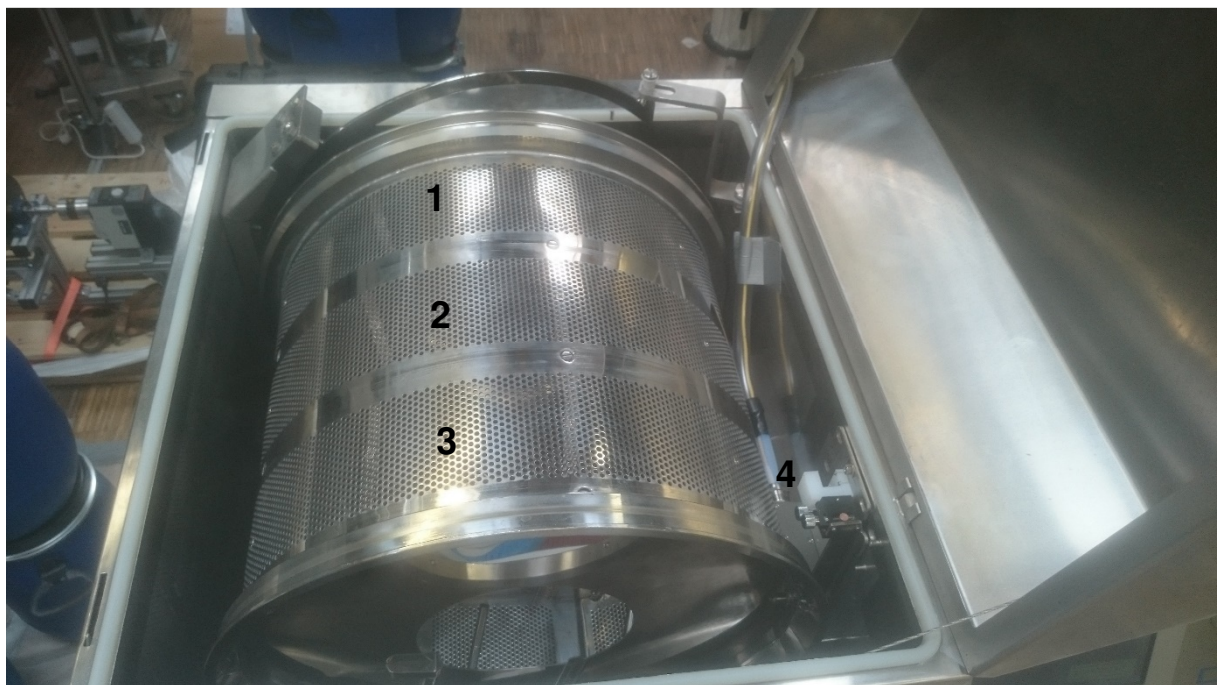
Figure 4: The rotating drum, with three chambers (1-3), inside the coater and the OCT-Sensor in a preliminary position (4).
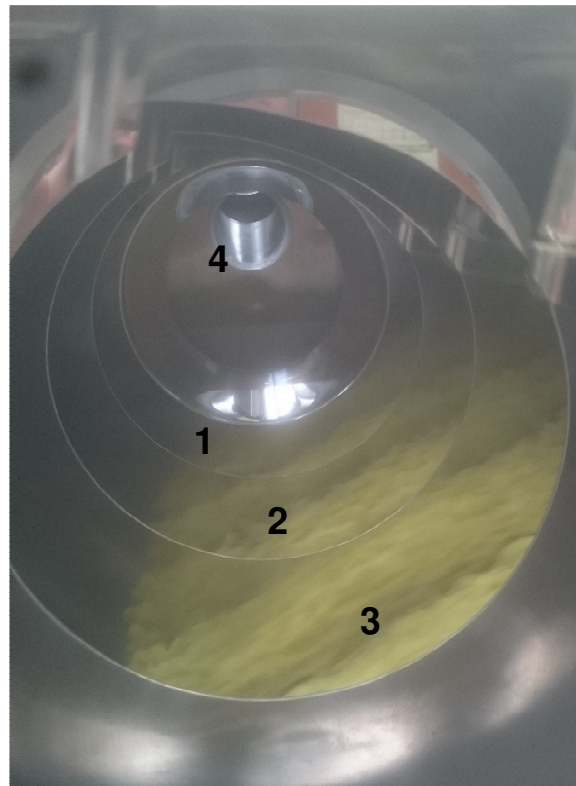
Figure 5: The three chambers (1-3) from the inside, including the tablet entrance (4).

Each chamber is equipped with a spraying nozzle, visible in Figure 6, manufactured by Schlick and with a bore diameter of 0.5mm, to distribute the coating suspension on the tablets. The nozzles are connected to three peristaltic pumps, which control the flow rate of the coating mass.

Figure 6: The three spraying nozzles (1-3).

The OCT sensor head is placed under the third and last chamber, beneath the perforated metal. This position, visible in Figure 7, is chosen after various test runs, that showed that the other, higher, positions only had very few tablets in the retrieved data. This was because

most of the tablets at this elevation were already sliding down again or not directly touching the drum anymore. The overall setup is shown and explained in Figure 8.

Figure 7: Final position of the OCT-Sensor (1) beneath the drum. The optical fibers are protected by surrounding hoses (2). To avoid dusting of the sensor window pressurized air is installed to protect the glass window (3).
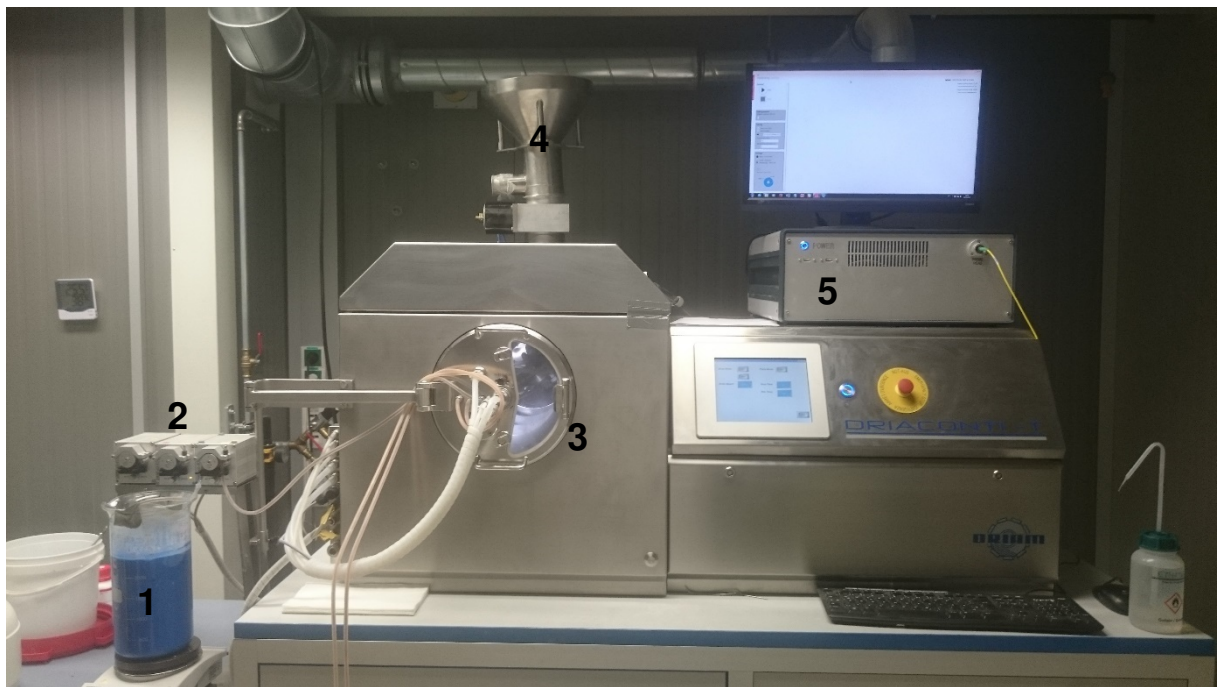
Figure 8: Full experimental setup during a coloring trial. The spraying suspension (1) is pumped by the peristaltic pumps (2) to the respective chambers (3). The tablets are added at the back (4), and the OCT-data is processed on the right top (5).

The pumps and the coater are steered via the touchscreen on the DRIACONTI-T® pharma LAB (Figure 9), while the OCT data acquisition (Figure 10) is performed on a separate PC, which is placed upon the drum coater.
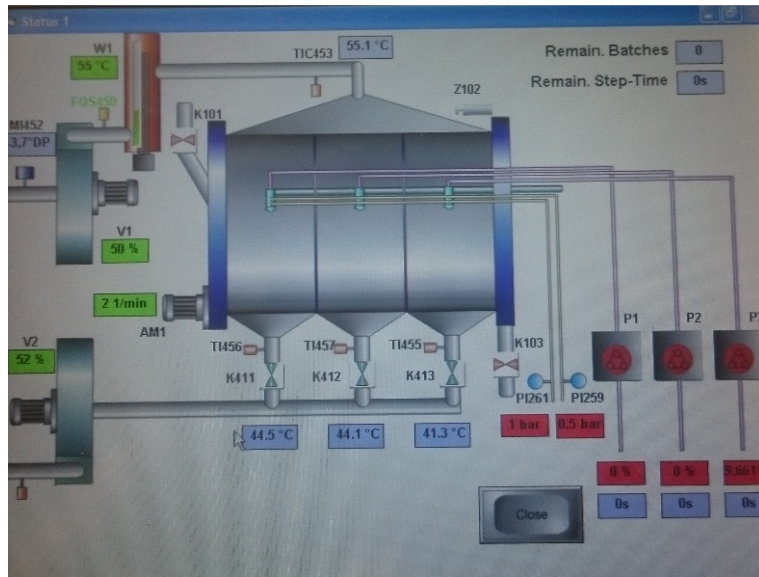
Figure 9: Touchscreen used to surveil and alter the process conditions.
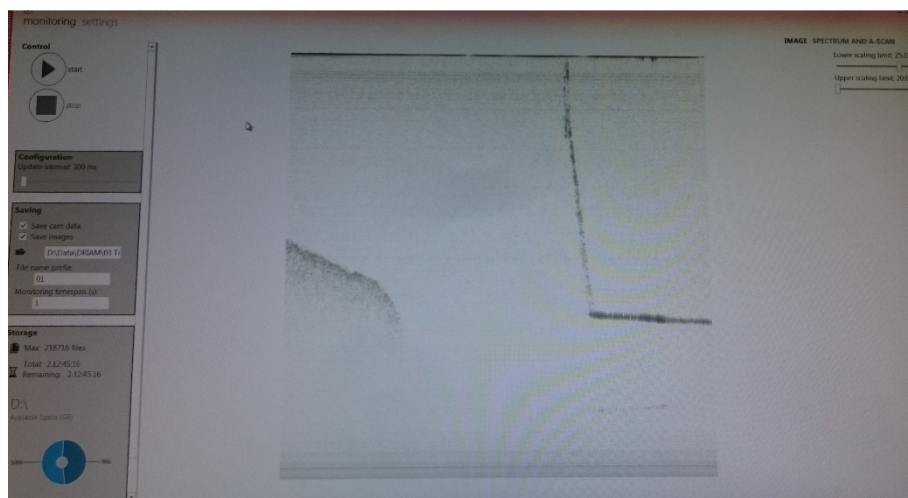
Figure 10: The data acquisition program OSeeT, running on the separate computer.

The tablets are moved from chamber to chamber and ejected by opening and closing flaps on the side walls of the chambers. Once a chamber change is started, the drum rotation slows down, the flaps open at the upmost point and perform a full rotation before closing again at the upmost point. The model of the drum coater and the flap positions are visualized in Figure 11, Figure 12 and Figure 13.
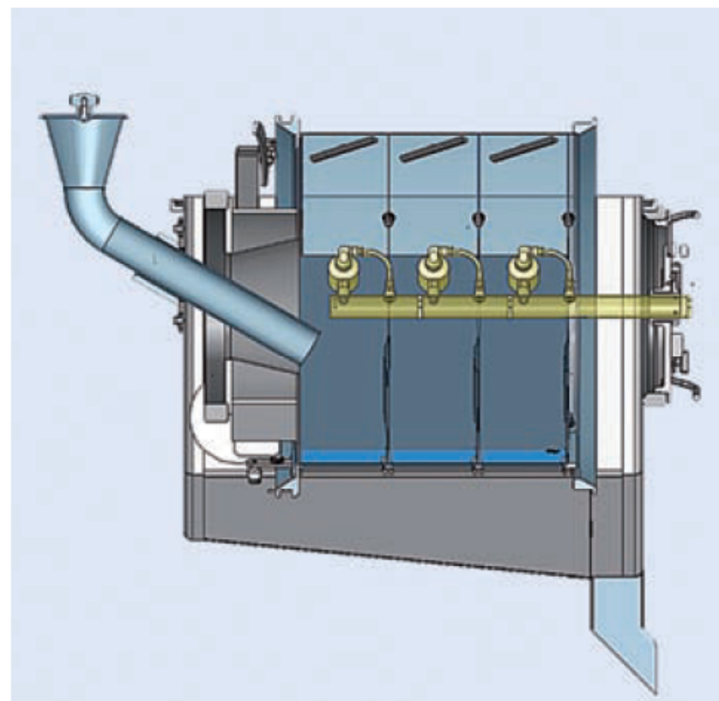
Figure 11: Model of the drum coater [27].
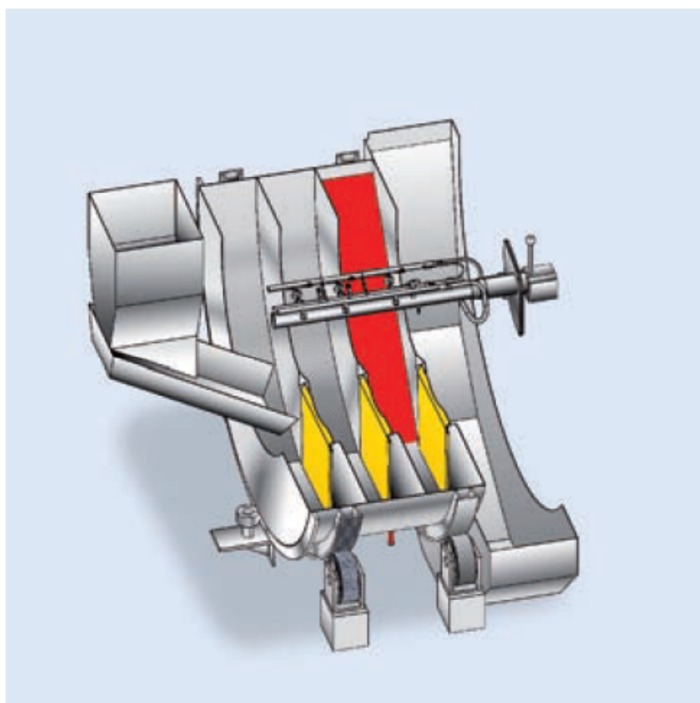
Figure 12: Model of the drum coater and the flap position during spraying [27].
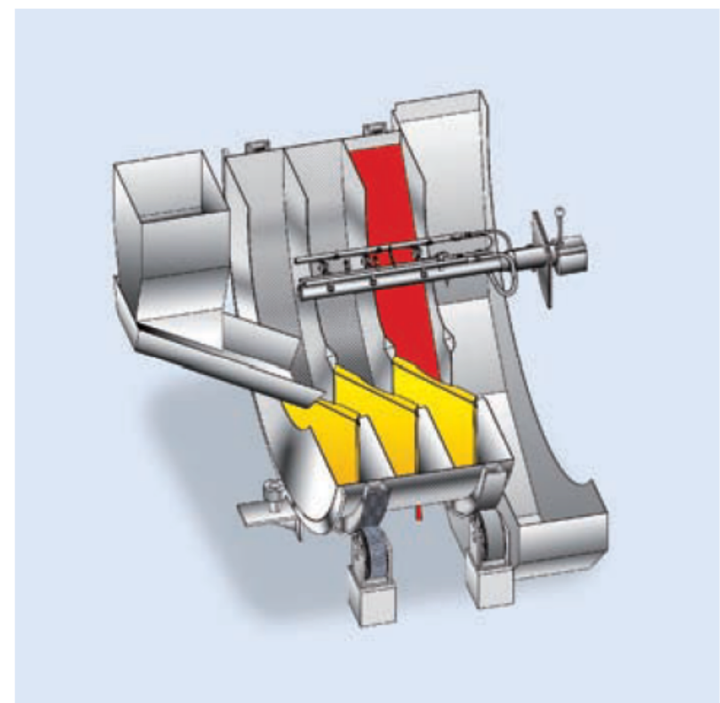
Figure 13: Model of the drum coater and the flap position during chamber exchange/ejection [27].

3.1.2. Used Materials

The tablets that are coated are ThromboASS® tablet cores, that were provided by G.L. Pharma. They consist of 100mg of acetyl salicylic acid, which serves as API and whose structure is shown in Figure 14, and an unknown amount of lactose-monohydrate, microcrystalline cellulose (MCC), silicon dioxide and starch.
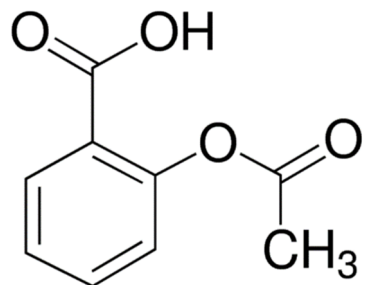
Figure 14: Structure of acetyl salicylic acid [28].

The used coating material is EUDRAGIT® L 30 D-55, an aqueous dispersion of an anionic copolymer, mainly made from methacrylic acid and ethyl acrylate, in a ratio of approximately 1:1. The molecular mass is about 320g/mol [29]. The molecular structure is shown in Figure 15.
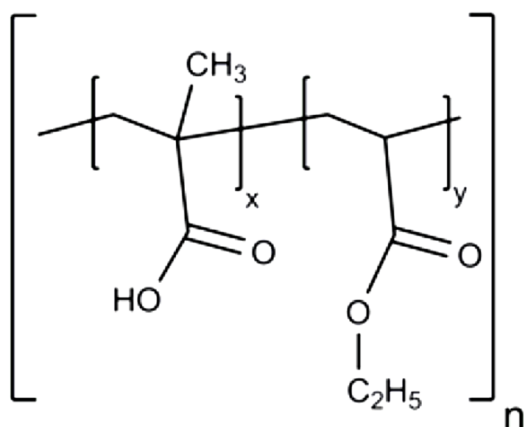
Figure 15: Molecular structure of the copolymer [29].

Triethyl citrate is used as a plasticizer. The molar mass is 276.29g/mol. The linear formula is $HOC(COOC_2H_5)(CH_2COOC_2H_5)_2$ and the structure is shown in Figure 16 [30].
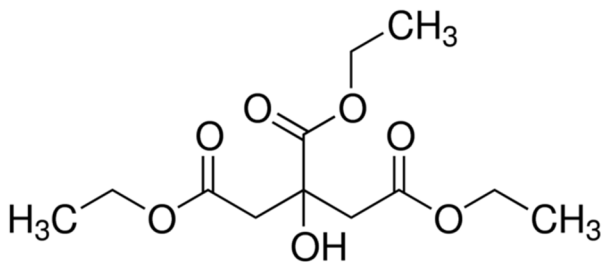
Figure 16: Structure of triethyl citrate [30].

Additionally, talcum is used as anti-tacking agent. The molecular weight is 379.29g/mol and the linear formula is $3MgO \cdot 4SiO_2 \cdot H_2O$ [31].

For the coloring trials indigocarmine and iron-oxide are used as dyes. Indigocarmine, with a molecular weight of 466.35g/mol, has the empirical formula $C_{16}H_8N_2Na_2O_8S_2$ and its structure is shown in Figure 17. The used red colorant is Iron-(III)-Oxide with the formula Fe_2O_3 and molecular weight of 159.69g/mol [23, 24].
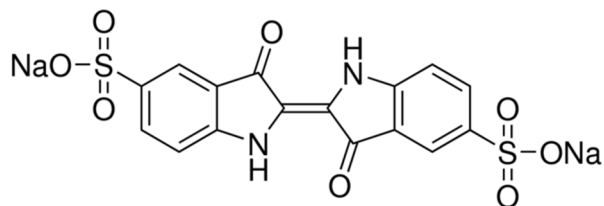
Figure 17: Chemical structure of indigocarmine [32].

3.2. Performed Experiments

In this section the conducted trials are described in more detail. First the process execution is described, followed by the different experiments that are conducted. The chapter is finalized by the encountered learnings.

3.2.1. Modus Operandi

First the tablets are filled into the desired chamber and the heating air is started at the wanted temperature, also the OCT-system is started in order to warm up. While the tablets are warmed up the materials for the coating suspension are prepared. The quantities and ingredients are listed in Table 3, which is a standard recipe from EVONIK and has already been used for previous tests with the OCT system.

Table 3:Ingredients and quantities inside the coating suspension [29].

Ingredient	Quantity	Dry substance
	[g]	[g]
EUDRAGIT® L30-D55	416.7	125.0
Triethyl citrate	12.5	12.5
Talc	62.5	62.5
Water	508.3	
Total	**1000**	**200**

First the talc and the triethyl citrate are homogenized in water. As there is no homogenizer available, they are strongly mixed by hand and then the suspension is added slowly into the EUDRAGIT® L30-D55 while being continuously stirred on a magnetic plate. Finally, the suspension is passed through a 0.5mm sieve and again continuously stirred [29].

Then the pumps are calibrated. Therefore, a pump speed is selected, and the throughput per minute is measured by collecting the pumped suspension in a beaker after the nozzle. If this amount equals the desired flow rate in g/min close enough, the throughput is measured two more times. If the rate deviates from the intended value, a new pump speed is calculated by interpolation and again tested. The calibration is finished when three consecutive runs are at or very close to the desired flow rate.

Then the nozzles are placed at their intended positions and the coating process as well as the OCT-surveillance are started. The suspension is sprayed until 140g dry coating, equaling 700g coating suspension and a tenth of the tablet mass, are brought onto the tablets. During the process the temperature in the chambers is noted numerous times. After the spraying is stopped, the tablets are left for 5 more minutes in the chamber to ensure that there are sufficient measurements of the tablets at maximum coating thickness taken by the OCT-equipment, before ejecting them into the product container.

Afterwards, the tablets are weighed to evaluate the amount of coating on the tablets, as well as the remaining coating suspension for the quantification of the spray loss. The pipes and the machine are cleaned with hot water and soap and dried for the next trial. A sample of 10 tablets per experiment is taken and measured concerning diameter and weight.

Also, offline OCT-measurements of these 10 tablets are performed to compare them to the on-line measurement. Therefore, every single tablet is placed under a 3D-OCT-sensor, which is adjusted until the tablet is clearly visible. The difference between on- and off-line measurements is visible in Figure 18 and Figure 19. While the tablet 3D-OCT sensor can be adjusted so that the tablet fills the whole measured length, this is not the case at the in-line 1D-OCT system, where also air and metal of the drum is visible.
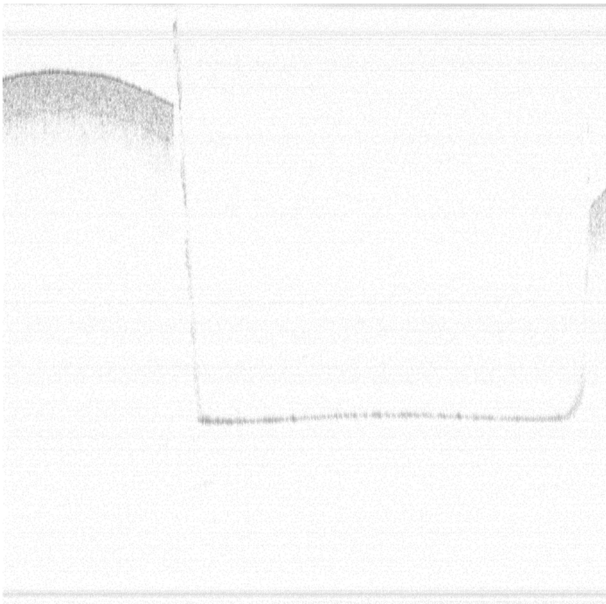
Figure 18: On-line measurement during experiment 1 of the DoE.
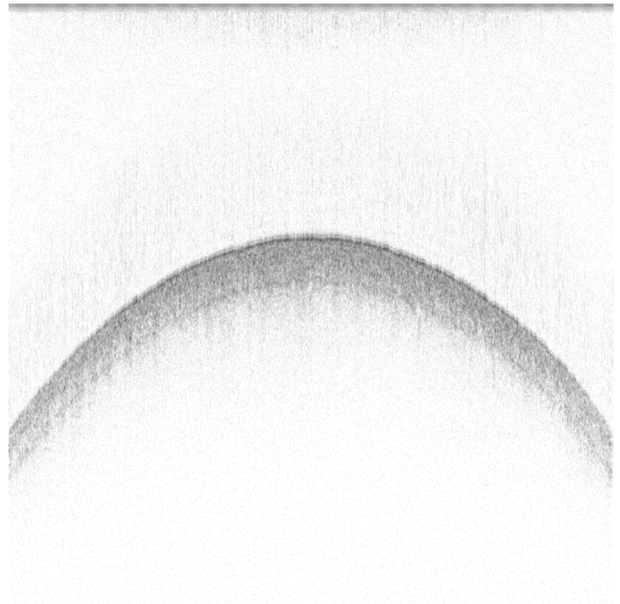
Figure 19: Off-line measurement of a tablet from experiment 1.

The off-line measurements are analyzed in ImageJ in a way that the number of pixels of the coating thickness is counted at three positions over each tablet. The pixels are divided by the total 1024 axial pixels and multiplied by the 1.6mm of the window length. By dividing this result through the refractive index, in this case 1.5, one gets the true coating thickness. For the inter tablet variability the standard deviation from the mean coating thickness of the 10 tablets is computed, whereas the intra tablet variability is calculated from the three different values per tablet. To compare the various intra variabilities, again the mean is calculated from the 10 different values. These calculations are performed within Microsoft Excel 2016.

3.2.2. Design of Experiments

In order to analyze the impact of different parameters, a full factorial Design of Expirements (DoE) is run at the coater, which is created in MODDE. For these trials, the coater is run in batch mode only, and only the third chamber was filled. The tablets are filled into the coater and moved to the third chamber where they are preheated to constant temperature. The DoE is listed in Table 4. The varied parameters are the flow rate in gram per minute per kg of tablets, the temperature of the inlet air and the pattern pressure at the spraying nozzle. The atomizing pressure, the drum speed and the tablet mass are kept constant throughout the experiments. The maximum and minimum values for the flow rate and the inlet temperature are taken from [29] and the pattern pressure is found by preliminary tests, where this pressure range proves to cause the least troubles concerning nozzle blockage. For the DoE, only the third chamber is used, as the OCT system is located there and otherwise no OCT-measurements from the first two thirds of the experiment would be available.

Table 4: List of the performed experiments with running order and parameters of the DoE.

Exp No	Exp Name	Run Order	Flow Rate	Inlet Temperature	Pattern Pressure	Atomizing Pressure	Drum RPM	Tablet mass
			[g/min/kg]	[°C]	[bar]	[bar]	[-]	[kg]
1	N1	1	3	45	1	0.7	22	1.4
2	N2	8	6	45	1	0.7	22	1.4
3	N3	3	3	60	1	0.7	22	1.4
4	N4	5	6	60	1	0.7	22	1.4
5	N5	7	3	45	1.6	0.7	22	1.4
6	N6	10	6	45	1.6	0.7	22	1.4
7	N7	6	3	60	1.6	0.7	22	1.4
8	N8	9	6	60	1.6	0.7	22	1.4
9	N9	2	4.5	52.5	1.3	0.7	22	1.4
10	N10	4	4.5	52.5	1.3	0.7	22	1.4
11	N11	11	4.5	52.5	1.3	0.7	22	1.4

3.2.3. Continuous Trial

For the continuous trial, 10 tablet-batches of 1400g are prepared as well as 8000g of the coating suspension. The tablets are preheated in an oven at 45°C. In contrast to the DoE, all chambers are used consecutively. When the first tablets enter the first chamber, the second 1400g are taken from the oven and poured into the filling hopper. After one third of the calculated coating time, the tablets change chamber and the new tablets are filled into the first chamber, being replaced by new tablets from the oven. T The process conditions equal the center-point trials from the DoE, being 52.5°C inlet temperature, 4.5g/min/kg flow rate and 1.3bar pattern pressure. The process is stopped shortly after the seventh batch enters the first chamber, due to persistent spraying problems because of nozzle blockage.

3.2.4. Color Trials

For the color trials two different colorants are chosen. Indigo carmine is chosen as blue, water soluble dye, while Iron-(III)-Oxide is used as red, insoluble coloring agent.

For the blue color trials, the indigo carmine is solved in the water prior to homogenizing the talc with the triethyl citrate. There are three runs performed, with 0.5w%, 2w% and 2.48w% of indigo carmine, based on the solid mass in the coating suspension. The 2.48 w% are the maximum soluble amount of indigo carmine in water for this recipe. An example of an indigo carmine spraying suspension is visible in Figure 20.

The red color trials are prepared similarly, therefore the iron oxide is added before the homogenization. The used concentrations are 0.5w%, 2w% and 10w% based on the solid mass content. The 10w% suspension is illustrated in Figure 21.

Figure 20: Indigo carmine spraying suspension (2w%)

Figure 21: Iron-(III)-oxide spraying suspension (10w%)

3.2.5. Results

In this subchapter, the obtained results are collected, starting with the DoE, followed by the continuous trial and finalized with the applicability of dyes for OCT-surveillance.

3.2.6. DoE

The results concerning the weight and the diameter of the tablet sample after the DoE experiments is shown in Table 5. It is visible that the values are very similar for the weight gain, while the diameter gain differs more, with experiment 1 being an outlier. A characterization of the coating process solely on these responses is not meaningful due to the similar results.

Table 5: Weight and diameter results of the DoE trials.

Experiment	Mean Weight	Weight Gain	Weight Standard Deviation	Mean Diameter	Diameter Gain	Diameter Standard Deviation
[-]	[g]	[g]	[g]	[mm]	[mm]	[mm]
Exp1	0.21473	0.01443	0.002528	7.8783	0.0614	0.00698
Exp2	0.21412	0.01382	0.002764	7.9112	0.0943	0.01227
Exp3	0.21434	0.01404	0.002614	7.9244	0.1075	0.01984
Exp4	0.21578	0.01548	0.001871	7.9552	0.1383	0.00908
Exp5	0.21449	0.01419	0.002243	7.9345	0.1176	0.01851
Exp6	0.21297	0.01267	0.001572	7.95	0.1331	0.02042
Exp7	0.21412	0.01382	0.002652	7.9291	0.1122	0.00720
Exp8	0.21319	0.01289	0.002319	7.9551	0.1382	0.02939
Exp9	0.2129	0.0126	0.002459	7.9575	0.1406	0.01486
Exp10	0.21326	0.01296	0.002991	7.9407	0.1238	0.01305
Exp11	0.21354	0.01324	0.002578	7.9484	0.1315	0.01933

The results are illustrated in Figure 22 and Figure 23. It can clearly be seen that there can be no statement made about the influences of the changed parameters, as the standard deviations of the different trials overlap. Also, the bottom outlier for the tablet diameters, experiment 1, does not show to weigh less as the other trials as is expected.

Diameter Gain of the DoE Experiments
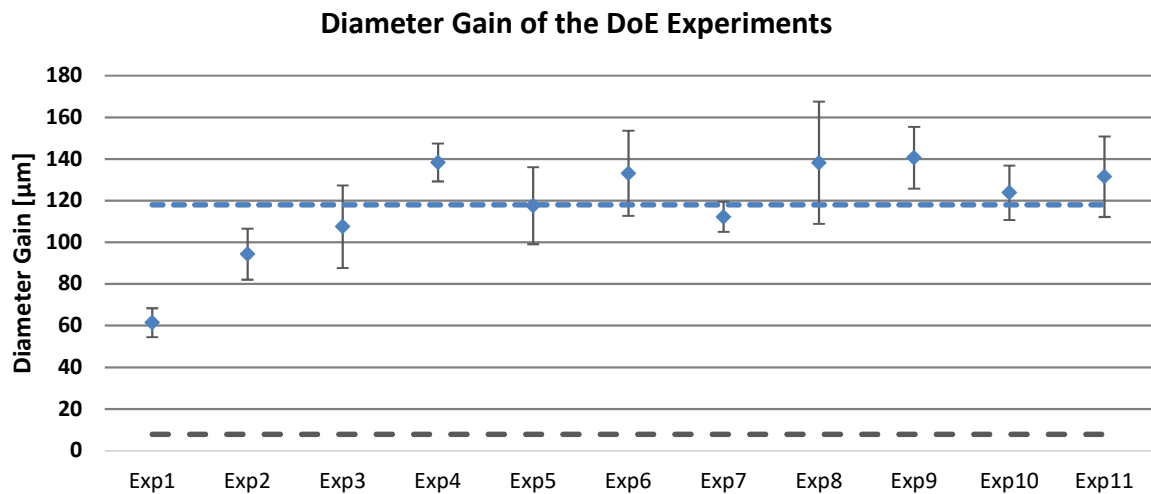
Figure 22: Results of the tablet diameter gain of the DoE visualized with the respective standard deviations. The blue dotted line is the mean over all trials and the grey dotted line is the standard deviation of the diameter of an uncoated tablet.

Weight Gain of the DoE Experiments
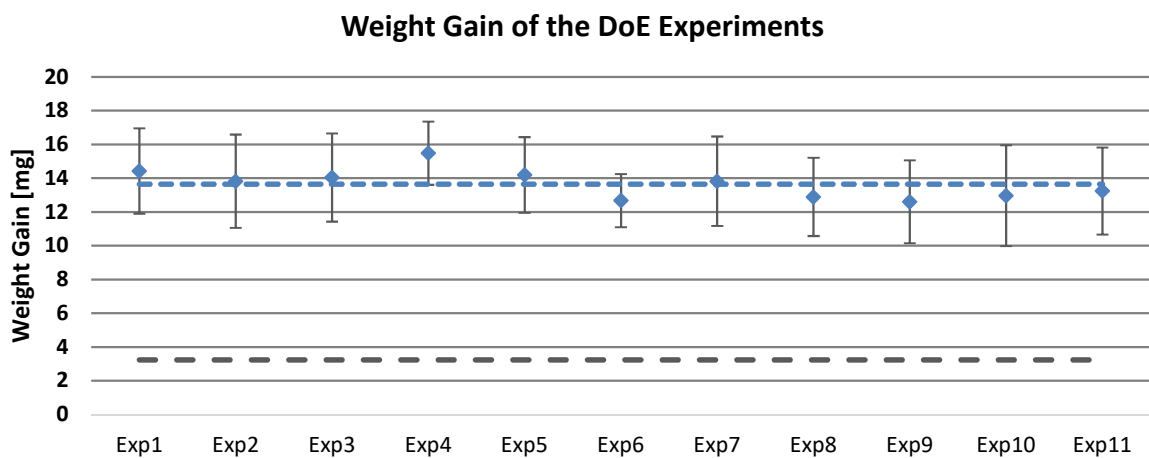
Figure 23: Results of the tablet weight gain of the DoE visualized with the respective standard deviations. The blue dotted line is the mean over all trials and the grey dotted line is the standard deviation of the weight of an uncoated tablet.

The coating thickness evaluation after the off-line measurements gives the results shown in Table 6. These results are compared with the total measured coating mass that is sprayed onto the tablet batch. There is a clear deviation at experiment 3, where there is a high coating thickness observed, while rather little coating mass is sprayed onto the tablets.

Table 6: Results of the off-line OCT coating thickness analysis of the DoE experiments, with intra and inter tablet standard deviation and coating mass.

Experiment	Coating Thickness	Inter Tablet Deviation	Intra Tablet Deviation	Coating Mass
[-]	[µm]	[µm]	[µm]	[g]
Exp1	77.53	1.937	2.131	99.5
Exp2	75.90	8.054	3.482	93
Exp3	80.80	6.769	3.467	82.4
Exp4	81.27	4.247	3.956	106.8
Exp5	75.90	4.086	3.346	99.2
Exp6	67.29	8.138	2.698	78
Exp7	71.91	1.440	3.041	90.4
Exp8	68.72	5.120	2.921	89.3
Exp9	72.43	3.748	3.052	88.4
Exp10	73.23	3.748	2.252	89
Exp11	72.40	4.050	2.127	91

The visualization of the coating thickness with inter and intra standard deviation in Figure 24 and Figure 25 shows the same characteristic. For a better comparability, the relative deviation of the results to the mean value was calculated. Most experiments follow the trend, but it can be observed that experiment 3 deviates clearly and also experiments 4,5 and 8 show differences of about 10%.
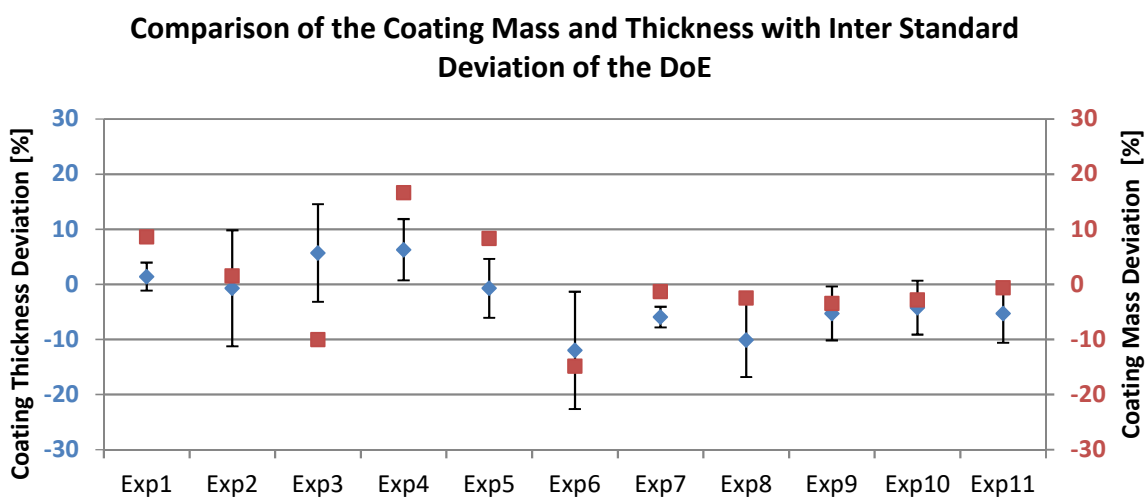
Figure 24: Results of the coating thickness with inter standard deviation, compared to the coating mass.

Comparison of the Coating Mass and Thickness with Intra Standard Deviation of the DoE
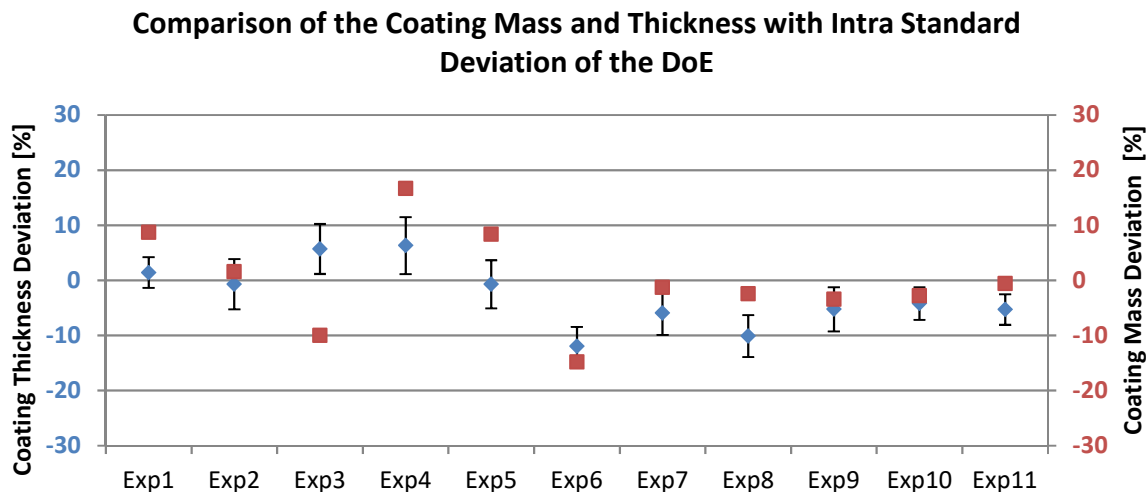
Figure 25: Results of the coating thickness with intra standard deviation, compared to the coating mass.

The analyzation of the two different coating thickness measurements gives the result shown in Figure 26. The results of the precision caliper were halved, to have the thickness of a single coating layer. It is shown that these results differ more than that of the 3D-OCT system, probably because of the huge impact of the operator on such a small scale. The OCT results are generally higher than those of the precision caliper. The inter standard deviation is used for the 3D-OCT values.

Comparison of the Coating Thickness Results of the DoE
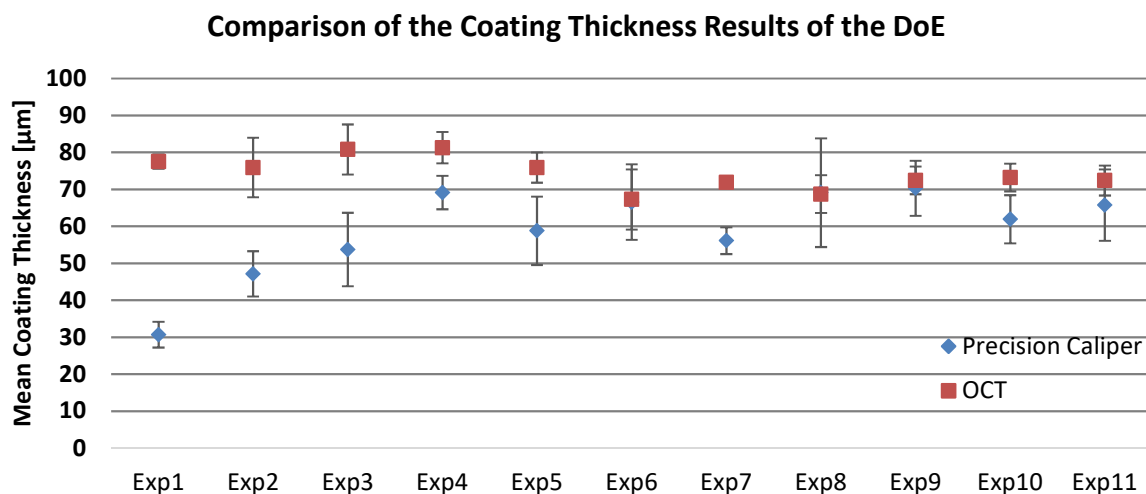
Figure 26: Comparison between the Thickness Measurements of the DoE.

Another investigated response is the temperature of the exhaust air from chamber three. The corresponding diagram is shown in Figure 27. The color scheme used is based on the inlet air temperature, being 45°C for the blue curves, 52.5°C for the green ones and 60°C for the orange colored experiments. The spraying was started at t=0, so the starting temperature should match the tablet temperature at the beginning rather closely. The fluctuations within

the data sets are caused by partial blockages of the nozzle, causing an inconsistent spraying pattern inside of the drum. For better analyzation, the time of the experiments has been normalized, as each spraying rate has its own process duration. As expected, the exhaust temperature is strongly connected to the inlet temperature. The only severe outlier is experiment 10, at which the nozzle was blocked nearly completely at the end of the experiment. Therefore, less solvent was evaporated, leading to an increase in temperature. Also at the other trials that show strong deviations (i.e. 5, 9, 11), the nozzles have been temporarily blocked at the respective times.
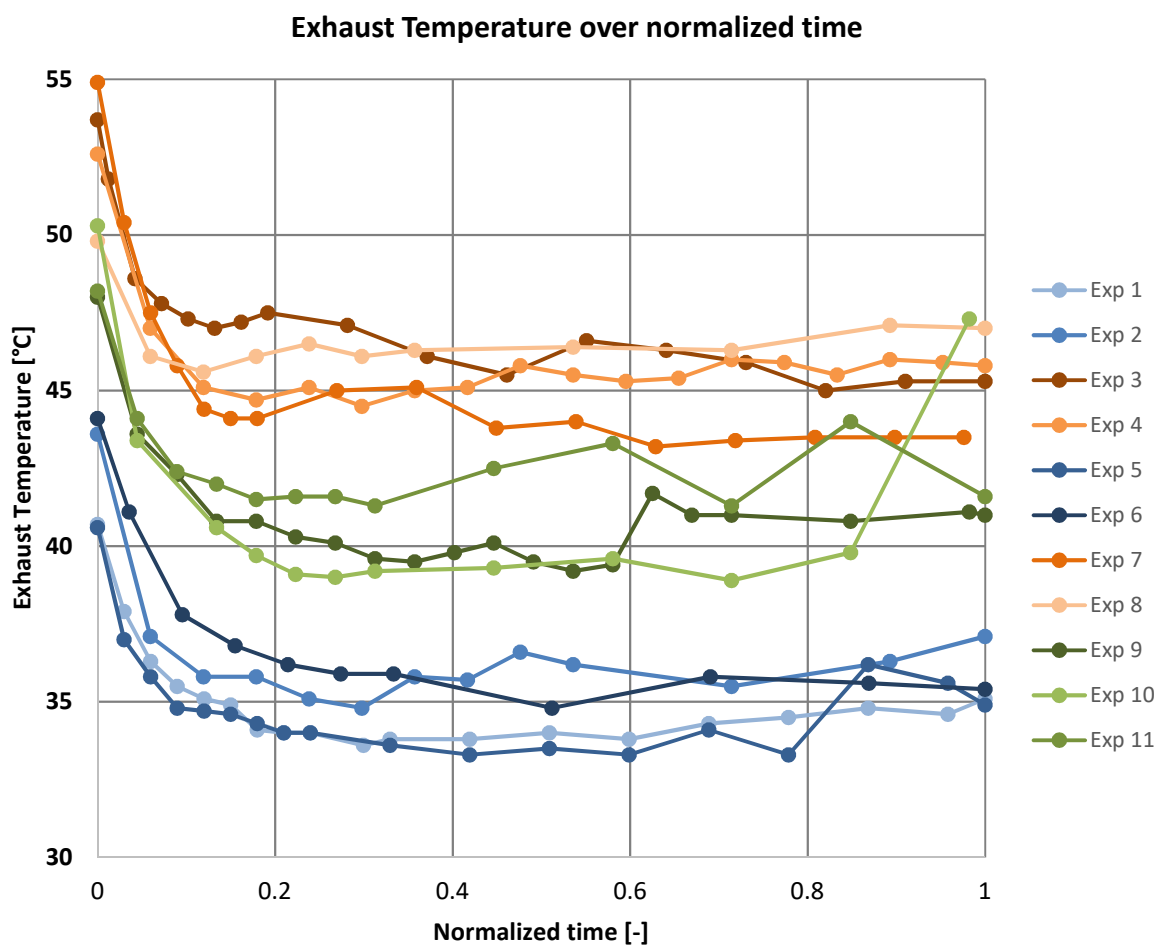
Figure 27:Exhaust temperature curves during the DoE experiments.

3.2.6.1. Continuous Trial

The tablets that are investigated after the continuous run give the values provided in Table 7. They are compared to the results of experiments 9, 10 and 11 from the DoE, as they were created under the same circumstances (52.5°C inlet temperature, 1.3 bar pattern air pressure, 4.5 grams coating per minute per kg of tablets).

Table 7: Weight and diameter results for the continuous run, compared to the DoE trials with the same parameters.

Batch	Mean Weight	Mean Weight Gain	Weight Standard Deviation	Mean Diameter	Mean Diameter Gain	Diameter Standard Deviation
[-]	[g]	[g]	[g]	[mm]		[mm]
Conti 1	0.21404	0.01374	0.001246	7.9567	0.1398	0.02584
Conti 2	0.21102	0.01072	0.002012	7.938	0.1211	0.01178
Conti 3	0.21041	0.01011	0.002450	7.917	0.1001	0.02708
Conti 4	0.2137	0.0134	0.003051	7.9472	0.1303	0.01457
Conti 5	0.2132	0.0129	0.002493	7.9555	0.1386	0.01062
Conti 6	0.21087	0.01057	0.002096	7.9376	0.1207	0.00521
Conti 7*	0.1978	-0.0025	0.002044	7.8497	0.0328	0.01564
Exp9	0.2129	0.0126	0.002459	7.9575	0.1406	0.01486
Exp10	0.21326	0.01296	0.002991	7.9407	0.1238	0.01305
Exp11	0.21354	0.01324	0.002578	7.9484	0.1315	0.01933

*Stopped due to nozzle blockage

It can be seen that the continuous trial shows much more fluctuations than the batch trials. This is especially visible in Figure 28 and Figure 29, where the results of the diameter and weight gain are compared between these runs. While experiments 9-11 show very similar characteristics, the continuous measurements deviate clearly and often show a broader standard deviation. This might be caused by tablet exchange between the different chambers, which was visible from time to time. It might also be that not all tablets are exchanged in one revelation of the drum and remain in their chambers due to sticking to the walls or drums, which could also be observed. Especially interesting is the result of the seventh sample, which shows a weight loss. This might be due to abrasion inside the drum, but it could also be that the measured tablets used to be below the average mass from the beginning, as they were sprayed for a very limited time. The spotted blue lines correspond to the mean values of the first 6 samples, while the grey spotted lines are the standard deviations of the uncoated tablets.

Diameter Gain of the Continuous Run
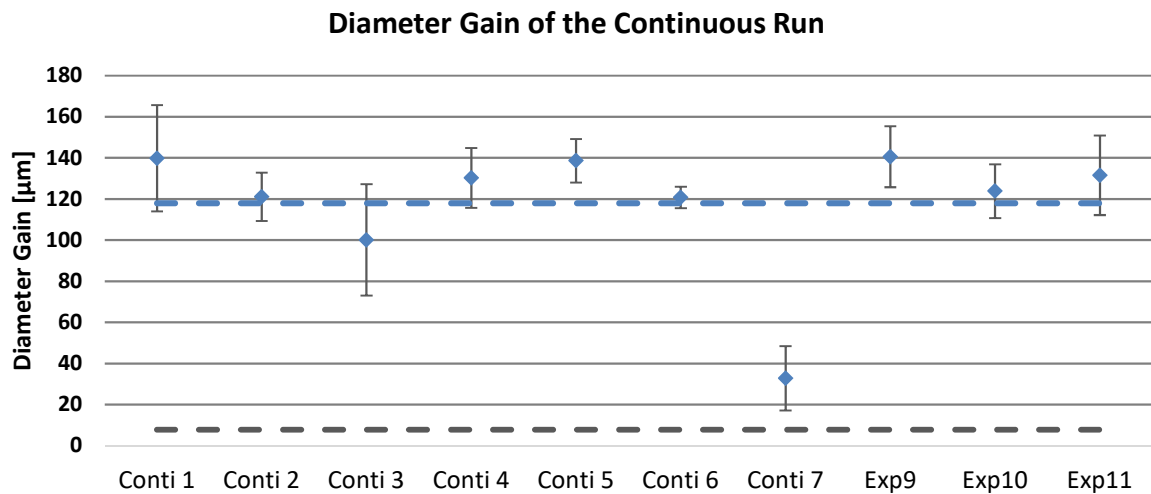
Figure 28: Diameter results for the continuous run, compared to the DoE trials with the same parameters. The blue dotted line is the mean over the first 6 batches and the grey dotted line is the standard deviation of the diameter of an uncoated tablet.

Weight Gain of the Continuous Run
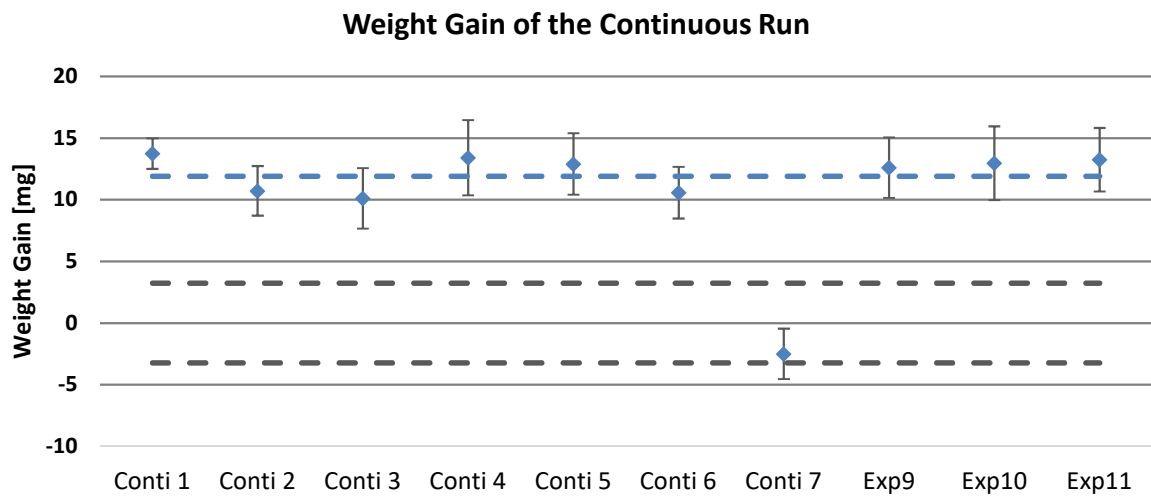
Figure 29: Weight results for the continuous run, compared to the DoE trials with the same parameters. The blue dotted line is the mean over the first 6 batches and the grey dotted line is the standard deviation of the weight of an uncoated tablet.

A similar result is achieved when the OCT data is compared. While the DoE trials are very similar concerning coating thickness, inter- and intra- deviation as well as coating mass, the different batches of the continuous run are different. Especially the inter tablet deviation and the coating mass vary severely, probably also caused by tablet exchange between the different chambers during the process. The results are collected in Table 8.

Table 8: Results of the off-line OCT measurements with inter and intra standard deviation, compared to the DoE trials with the same parameters.

Batch	Coating Thickness	Inter Tablet Deviation	Intra Tablet Deviation	Coating Mass
[-]	[µm]	[µm]	[µm]	[g]
Conti 1	71.84	5.506	2.168	74.5
Conti 2	65.80	3.335	2.982	94
Conti 3	56.25	11.279	4.026	100.5
Conti 4	61.60	13.213	4.011	78.3
Conti 5	68.89	3.804	3.359	78.7
Conti 6	61.98	4.593	4.074	75.5
Conti 7	12.05	3.062	2.247	8.4
Exp9	72.43	3.748	3.052	88.4
Exp10	73.23	3.748	2.252	89
Exp11	72.40	4.050	2.127	91

In Figure 30 and Figure 31 the results, excluding the seventh sample, are plotted with the corresponding intra and inter tablet standard deviation, with the relative deviation to the mean value of the first six samples. It is visible that the coating mass trend does not match the coating thickness, also there is no result that matches the three DoE experiments closely. However, the intra standard deviation is rather low, so the coated tablets show a good homogeneity.
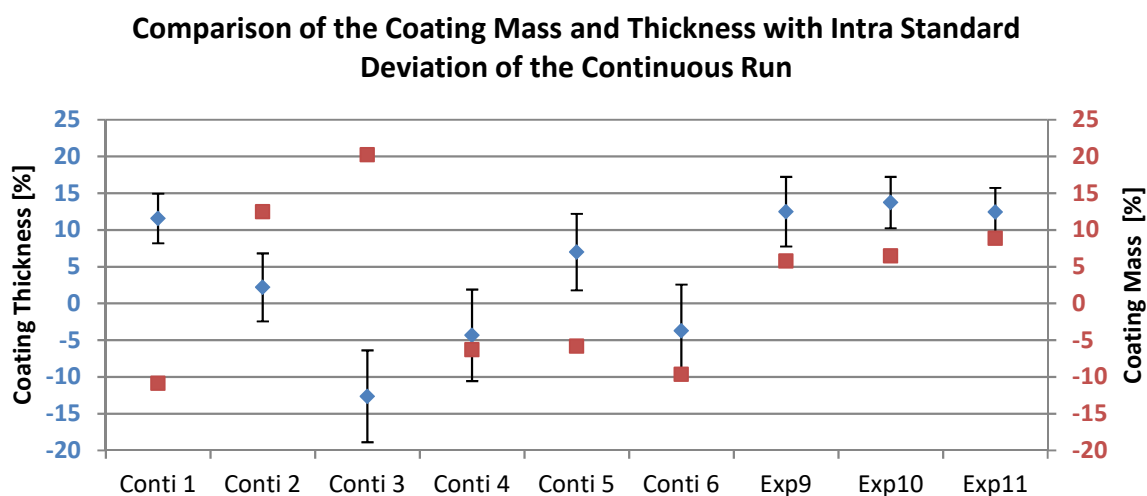
Figure 30: Comparison of the coating mass and the off-line OCT measurements with intra standard deviation, compared to the DoE trials with the same parameters.

When looking at Figure 31 it can clearly be seen that the inter tablet standard deviation is very high for some of the continuous samples, especially the third and fourth batch show strong fluctuations within the different measurements, but could also be caused by unclear OCT measurements. A possible cause to this phenomenon is also the tablet exchange during the process. As a large inter standard deviation does not correspond to high intra standard deviations, it might be indicated that the tablets within a sample have been coated differently long.
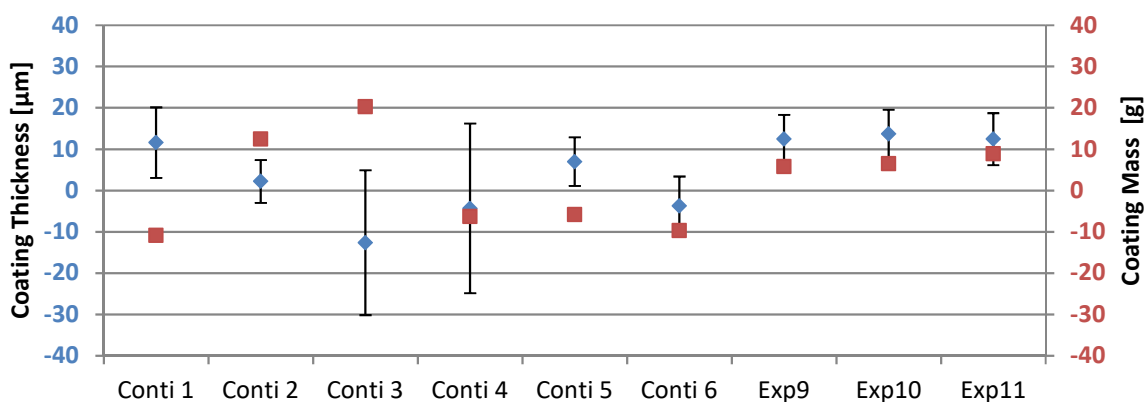
Figure 31: Comparison of the coating mass and the off-line OCT measurements with inter standard deviation, compared to the DoE trials with the same parameters.

Figure 32 shows the comparison between the 3D-OCT and the precision caliper results of the continuous run. As in the DoE results, the results of the 3D-OCT system are generally larger. However, it is nicely visible that the trend of both results is the same.
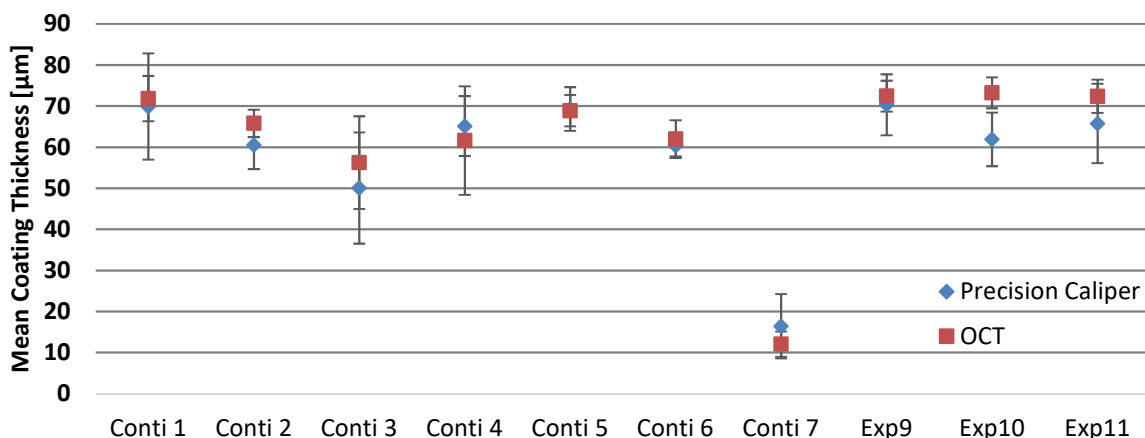
Figure 32: Comparison between the Thickness Measurements of the Continuous Run.

In Figure 33 the temperature courses over the process time are depicted. It can be easily seen when the tablets first enter the respective chambers, as the temperature drops extensively. Also the chamber exchanges are visible by short temperature deviations. At the end of the process, when the nozzle blockage started to begin, the temperature rises at chamber 1 and chamber 2, due to no new coating suspension that has to be evaporated. It remains unclear why the temperature of chamber 2 is below the temperature of the other two chambers. One possibility might be that the spraying rate of the second nozzle was higher than those of the other two.
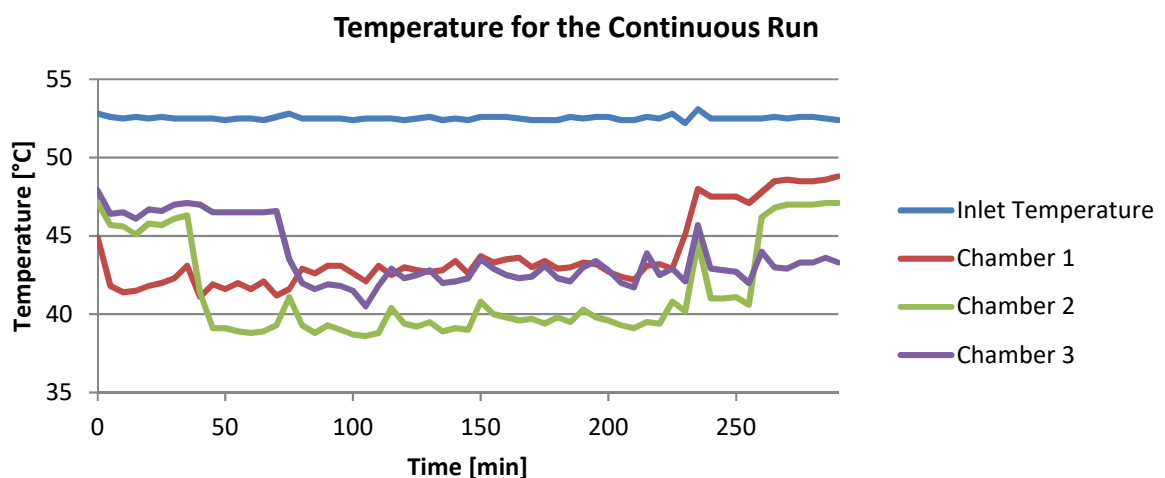
Figure 33: Temperature over the course of time for the continuous run.

3.2.6.2. Color Trials

In order to be able to evaluate the practicability of OCT-measurements for indigo carmine and iron-(III)-oxide the tablets of the various runs are analyzed off-line and visually. In Figure 34 the different colors corresponding to the formulation can be seen.
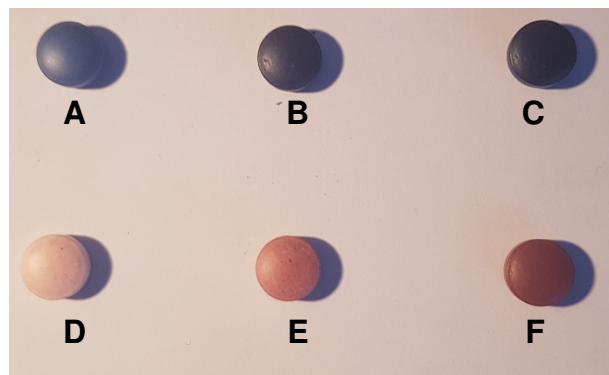
Figure 34: Picture of the 0.5w%(A), 2w%(B) and 2.48w%(C) Indigocarmine tablets with the 0.5w%(D), 2w%(E) and 10w%(F) Fe2O3 tablets.

For the indigo carmine trials, it is visible that there is no difference between the 0.5w% (Figure 35), 2w% (Figure 36) and 2.48w% (Figure 37) trials, and that the coating thickness can be evaluated using OCT-means.
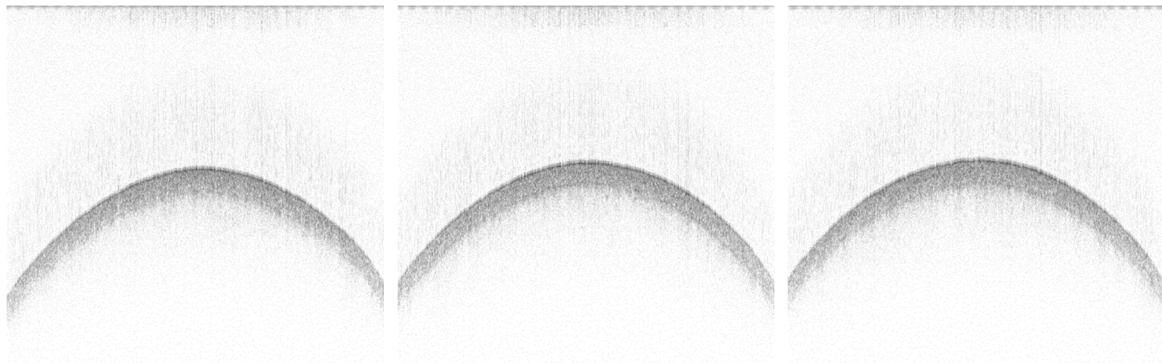
Figure 35: Off-line OCT measurement of the 0.5w% Indigocarmine trial.

Figure 36: Off-line OCT measurement of the 2w% Indigocarmine trial.

Figure 37: Off-line OCT measurement of the 2.48w% Indigocarmine trial.

In contrast to the soluble dye, the solid dye iron-(III)-oxide shows different characteristics. As shown in Figure 38, Figure and Figure 40 the coating thickness looks smaller with increasing colorant content. This is probably caused by extensive scattering of the light and therefore a very small penetration depth.
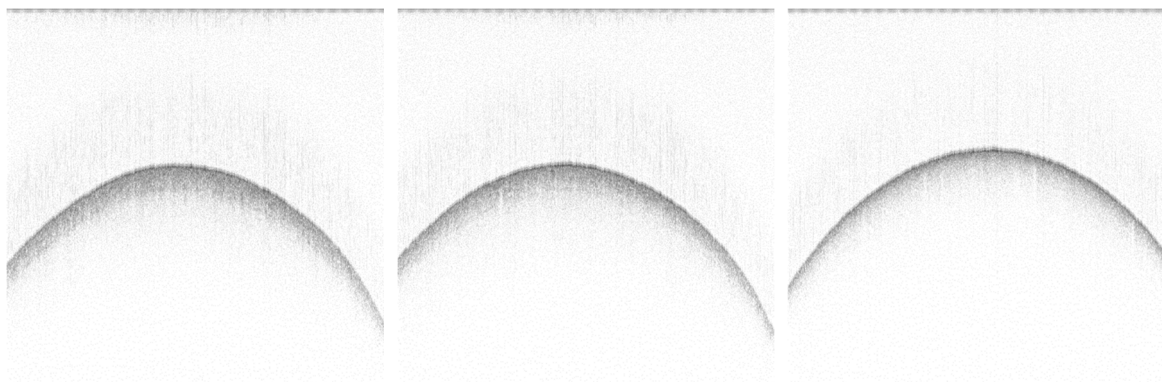
Figure 38: Off-line OCT measurement of the 0.5w% Fe_2O_3 trial.

Figure 39 Off-line OCT measurement of the 2w% Fe_2O_3 trial.

Figure 40 Off-line OCT measurement of the 10w% Fe_2O_3 trial.

Concluding it can be said that for colorant trials soluble dyes seem to be more promising concerning the evaluability via OCT. Therefore, future trials should be performed with water soluble colorants.

3.2.7. Possible Improvements

This subchapter summarizes the possible ameliorations that are arising during the experiments and the evaluation. First the sensor head fouling is discussed, followed by the nozzle blockage. This subchapter is concluded with general thoughts on the experimental setup and the modus operandi.

3.2.7.1. Sensor Head Fouling

During the progress of the DoE there was a clear worsening of the quality of the OCT-data. This is illustrated by Figure 41. The cause of the inferior quality data is shown in Figure 42. Over the numerous trials, coating suspension was sprayed onto the sensor head of the OCT measuring system, despite the installed pressurized air stream, due to a movement of the cleaning air stream during the processes. This caused a drastic loss of light intensity. As the data of several trials was too bad for analyzation, the experiments 2, 6 and 8 had to be repeated after the cleaning of the sensor head.
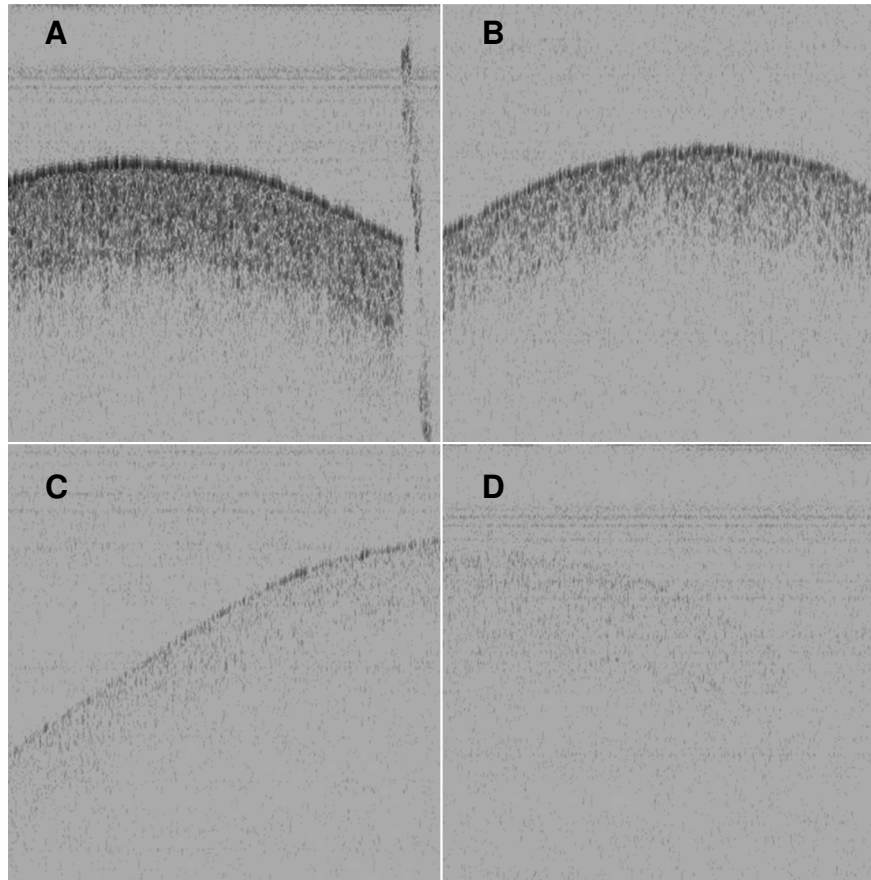
Figure 41: OCT-Pictures of the 1ˢᵗ(A), 4ᵗʰ(B), 8ᵗʰ(C) and 9ᵗʰ(D) run.
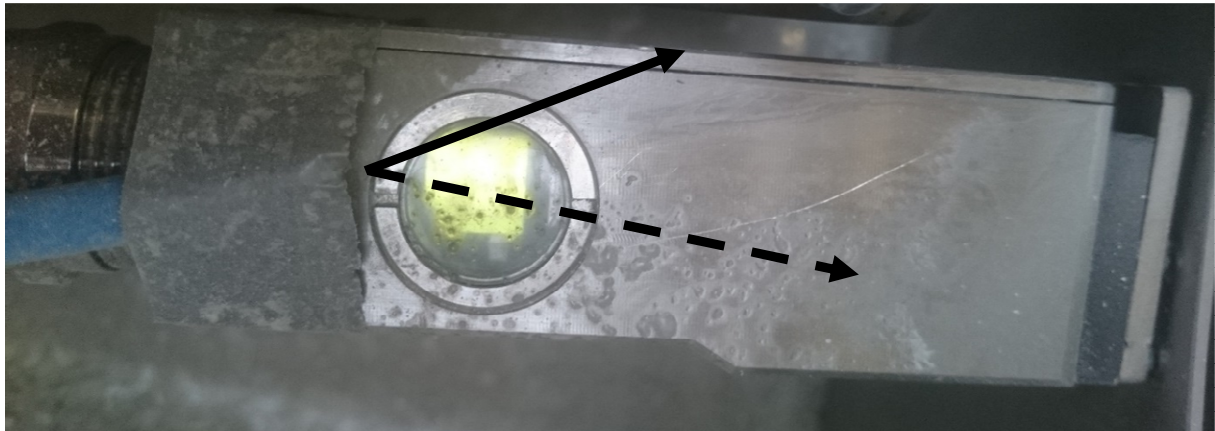
Figure 42: Dirty sensor head with desired (dotted arrow) and actual (continuous arrow) air stream direction.

3.2.7.2. Nozzle Blockage

It is visible during the experiments that some of the coating material blocks the nozzle partially or completely, as shown in Figure 43. Normally these blockages are blown away after a few seconds, but prove to be problematic especially for the continuous trial, as it has to be stopped due to persistent blockage. This might be caused by a non-homogenous coating suspension with a broad particle size distribution, or a too small nozzle bore. As the nozzle bores described in [29] have a diameter of 1.2mm instead of the used 0.5mm, the reproduction of the experiments with a larger bore is advised.

Figure 43: Blocked nozzle.

3.2.7.3. Experimental Setup

For further experiments, it might be of advantage to install an air conditioning (AC) unit before the air enters the coater, as there was no information concerning the drying capacity or humidity of the incoming airstream. To achieve a high reproducibility of the experiments it is vital to have comparable humidity over the course of the experiments.

Additionally, the utilization of a homogenizer is strongly recommended, as the obtained OCT-data does not show two distinct layers, as would be preferable. This is probably caused by the diffraction of the materials in the coating suspension or a wrong formulation. To visualize this effect, a tablet coated in the scope of this thesis (Figure 44) is compared to an off-line OCT image taken from a commercially available tablet, coated with the same ingredients (Figure 45).
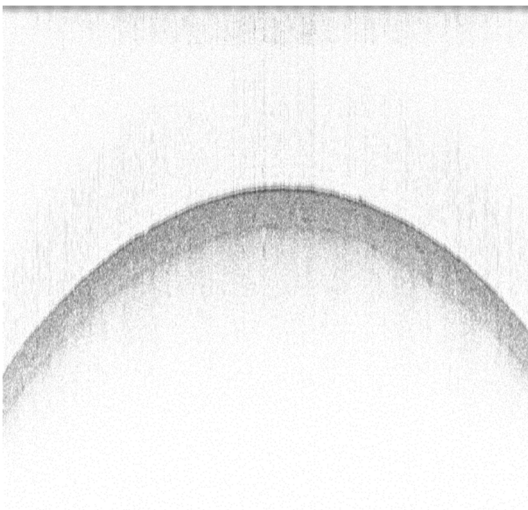
Figure 44: OCT image of a tablet from Experiment 1.
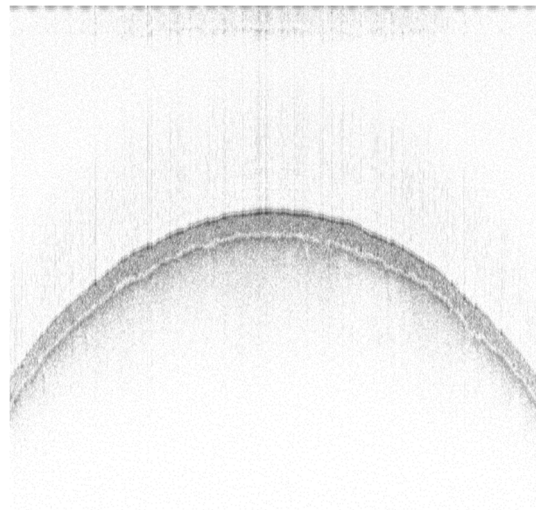
Figure 45: OCT image of a commercially available ThromboASS 100mg tablet.

Another aspect that should be altered is the positioning of the OCT-sensor head. Due to the non-sphericity of the drum only very few tablets are visible in the correct distance to the OCT-sensor head. Instead, there are a lot of pictures with mirrored tablets and the metal drum. As the eccentricity is very hard to influence and will probably even get worse with larger drums, a new system should be implemented inside of the coater, to enable fine adjustment of the sensor head to minimize the pictures outside of the optimal range. However, this might prove to be very time-consuming and expensive. Therefore, alternative approaches are to increase the measurement length or adapt the image taking rate to minimize the influence of the eccentricity.

3.3. Data Evaluation

This subchapter deals with the evaluation of the obtained data. First the results of the coating thickness and coating mass are compared to a mathematical model. Afterwards all parameters and responses are analyzed within MODDE 11 to find the most suitable coating conditions for the coating process.

3.3.1. Observed vs. Calculated Coating Thickness

To be able to find out if the obtained results are meaningful the results have been compared to a mathematical model. Therefore, the density of a mixture of the solid compounds of the coating suspension is calculated in two ways. The used densities for the first method are given in Table 9. This calculation is strongly idealized and just used for a rough estimation.

Table 9: Used densities for the calculation

Material	Bulk Density	Mass	Volume
[-]	[kg/m³]	[kg]	[m³]
Eudragit	980 [34]	125	0.12755102
Talkum	2700 [35]	12.5	0.00462963
Triethyl citrate	1140 [30]	62.5	0.05482456
Solid Content Suspension	**1069.488911**	**200**	**0.18700521**

The second method to calculate the film density is to prepare 50g of coating suspension and measuring the volume. By subtracting the volume of the 40g of water at 20°C, which has to be evaporated, a volume of the solid compounds can be calculated. The mass of the solid contents (10g) divided by the remaining volume gives an estimate for the density of the coating film. This measurement is performed three times and the used density is the mean value over the trials. The obtained densities are 1.524g/ml, 1.571g/ml and 1.457g/ml, resulting in the mean value 1.517g/ml.

For the coupling of coating thickness and coating mass a mean number of tablets is calculated by dividing the 1400g of total mass by the 200.3mg, which is the mean tablet weight of 10 uncoated tablets. The result is rounded to the nearest digit, giving approximately 6990 tablets. With the characteristic lengths shown in Figure 46 and the consecutive equations a trend curve is created.
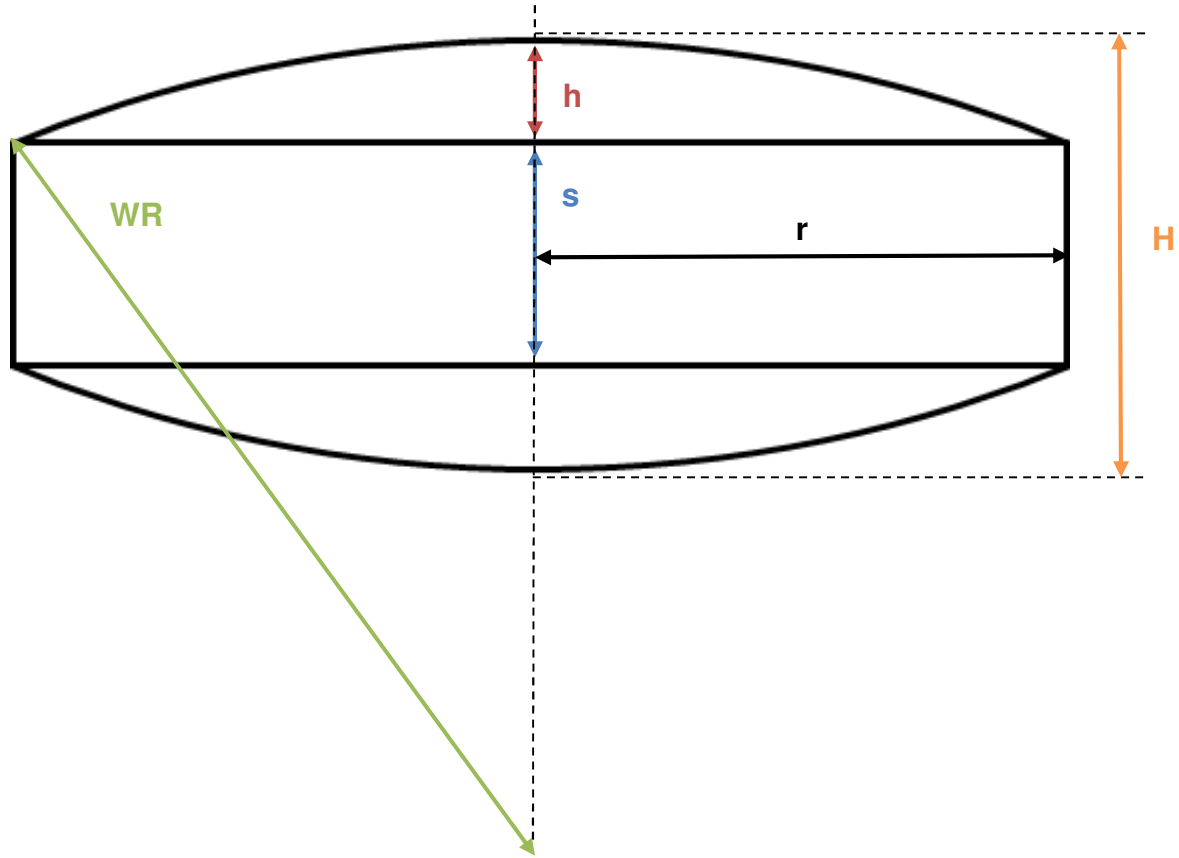
Figure 46: Diagram with characteristic lengths of biconvex tablets [26, 27].

$$h = WR - \sqrt{WR^2 - r^2} \tag{6}$$

$$H = 2h + s \tag{7}$$

$$V = \pi(r^2 s + r^2 h + 3h^3) \tag{8}$$

$$m = \rho * \pi(r^2 s + r^2 h + 3h^3) \tag{9}$$

$$m = \rho * \pi * ((r + x)^2 s + (r + x)^2(h + x) + 3(h + x)^3) \tag{10}$$

By multiplying the volume of a tablet with the calculated density the total mass of a tablet (consisting just out of coating) is calculated according to equation 9. With the coating layer thickness x the new mass of each tablet is computed as in equation 10. By subtracting (9) from (10), the coating mass gain of certain coating thicknesses can be found, resulting in a total mass gain for each batch when multiplied by the number of tablets. The results from the 3D-OCT system, shown in Figure 47, show to be between the two calculated densities, except for experiment 3. As there is no information concerning the true film density of the

used coating, this is a good method to estimate the coating thickness when the coating mass is given or vice versa.

Comparison between the 3D-OCT and the calculated Coating Thickness
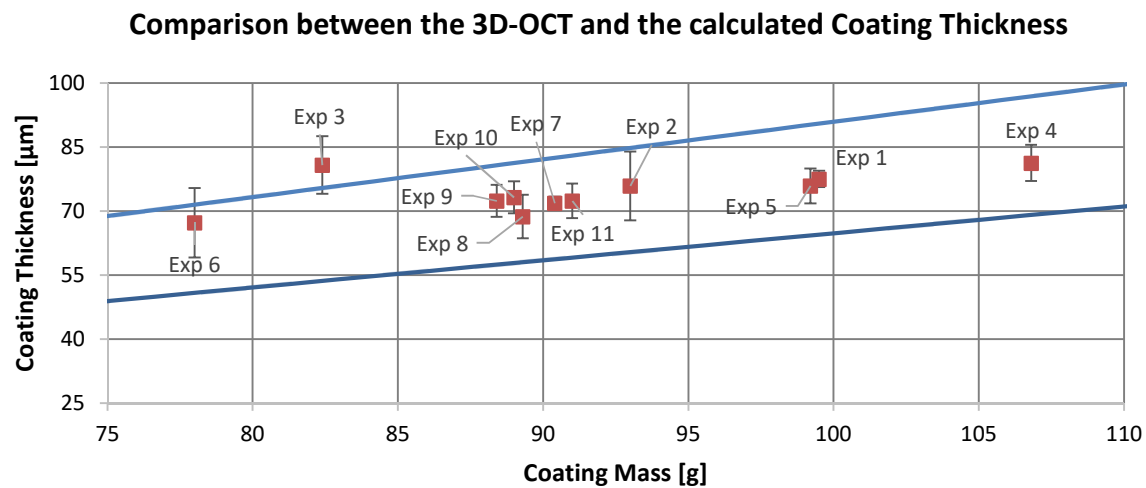
Figure 47: 3D-OCT measured vs. calculated coating thickness over coating mass. The upper blue line corresponds to the density calculated out of the bulk densities and the lower blue line corresponds to the volume based calculation.

In Figure 48 the measurements of the precision caliper are compared to the model. Most results are still between the two densities, however there are more outliers. This might be caused by the inaccuracies when manually analyzing thicknesses of such small scale. To evaluate how good the data fits the model it is advised to gather information about the true density of the film and to analyze the refractive index of the coating.

Comparison between the Precision Caliper and the calculated Coating Thickness
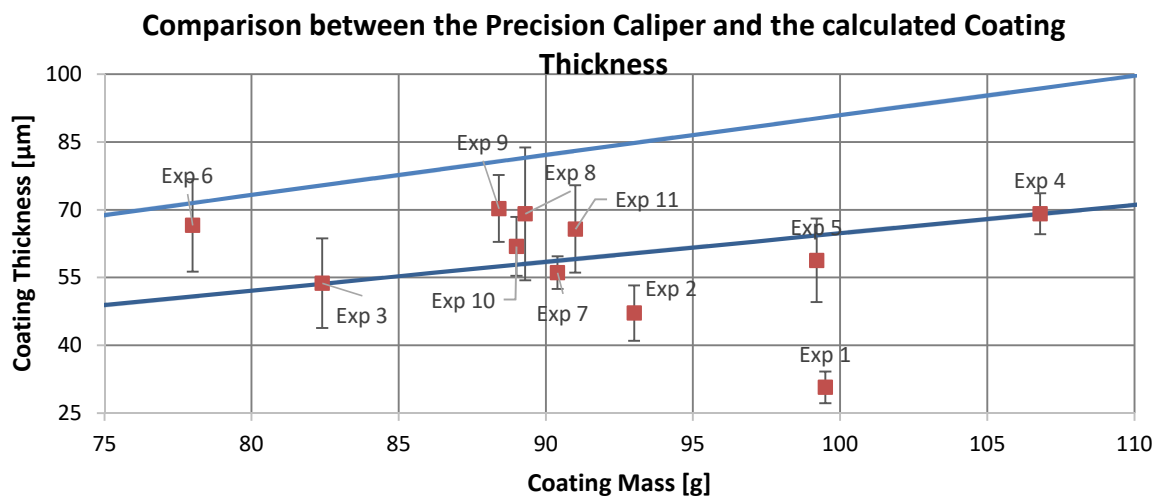
Figure 48: Precision Caliper measured vs. calculated coating thickness over coating mass. The upper blue line corresponds to the density calculated out of the bulk densities and the lower blue line corresponds to the volume based calculation.

3.3.2. Analysis within MODDE 11

The evaluation of the DoE is vital to find suitable coating conditions for future processes. Thereby it is possible to design processes to reduce spray loss, maximize coating thickness and uniformity or find the best parameters for fast coating processes. To be able to analyze the influences of the different parameters, the results of the DoE experiments are entered in MODDE 11. As responses, the coating mass, the spray loss, the tablet weight, the tablet diameter, the coating thickness, the inter- and intra- standard deviation of the coating and the exhaust temperature are chosen. The coating thickness and tablet diameter were chosen because the results were equivalent to an analysis with the respective gains. The results are collected in Table 10. Extra to the already mentioned responses, the spray loss is calculated via dividing the coating mass by the solid content of the sprayed coating suspension. The exhaust temperature is the mean temperature of the air after chamber 3, after the system has reached a steady state. Experiment 3 was excluded prior to data evaluation, as the results are clearly deviating from the expected values and therefore interfered with a meaningful interpretation.

Table 10:Collected responses for the data analysis in MODDE 11.

	Coating Mass	Spray loss	Tablet Weight	Tablet Diameter	Coating Thickness	Inter Deviation	Intra Deviation	Exhaust Temperature
	[g]	[%]	[g]	[mm]	[µm]	[µm]	[µm]	[°C]
N1	99.5	26.84	0.21473	7.8783	77.53	1.937	2.131	35
N2	93	40.38	0.21412	7.9112	75.90	8.054	3.482	37.1
N3	82.4	38.98	0.21434	7.9244	80.80	6.769	3.467	45.3
N4	106.8	24.79	0.21578	7.9552	81.27	4.247	3.956	45.8
N5	99.2	19.74	0.21449	7.9345	75.90	4.086	3.346	34.9
N6	78	39.25	0.21297	7.95	67.29	8.138	2.698	35.4
N7	90.4	32.46	0.21412	7.9291	71.91	1.440	3.041	43.5
N8	89.3	40.7	0.21319	7.9551	56.01	3.204	4.277	47
N9	88.4	39.24	0.2129	7.9575	72.43	3.748	3.052	41
N10	89	30.15	0.21326	7.9407	73.23	3.748	2.252	40
N11	91	33.18	0.21345	7.9484	72.40	4.050	2.127	41.6

In Figure 49 the summary of fit for the DoE is shown. It is visible that the obtained data does not fit the model very well, especially the spray loss, the tablet weight and the intra deviation are not depicted in a good manner. This might be explained with the nozzle blockages for the spray loss and the intra deviation. The intra deviation could also be depicted wrongly, as there are only three, user dependent, measurements per tablet. As the standard deviation of the uncoated tablet weight is about one fourth of the weight gain during the process, this

might have caused a bad model fit. The same explanation is valid for the diameter, although the standard deviation of the diameter is only about one fifteenth of the diameter gain.
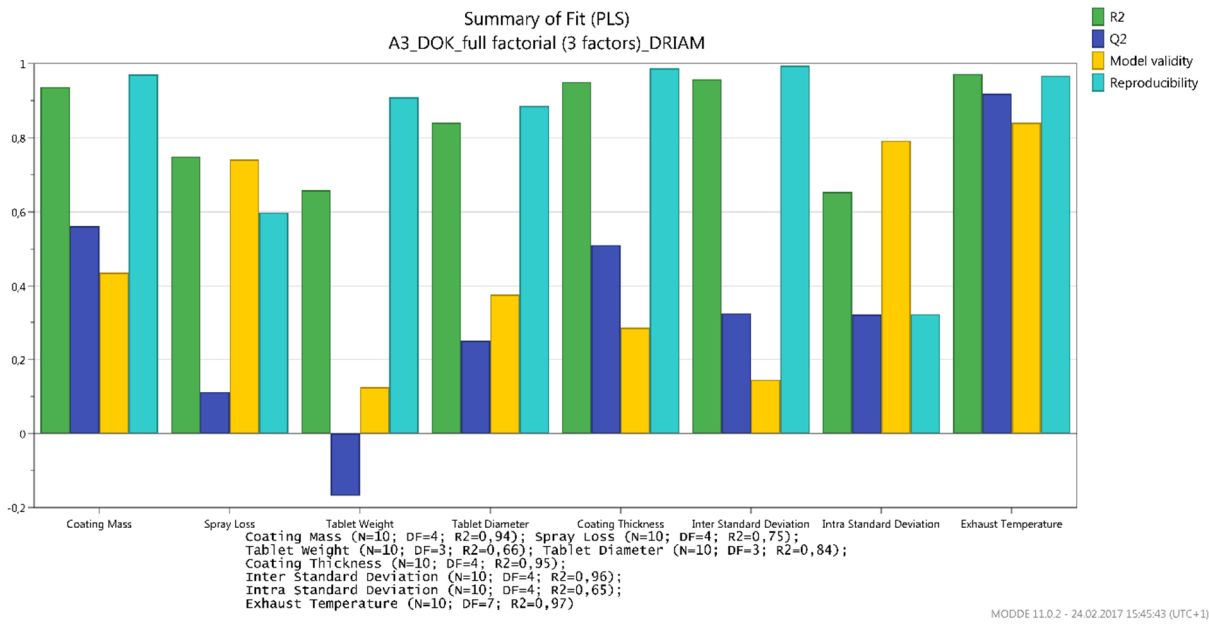
Figure 49: Summary of Fit of the obtained data in MODDE 11.

For the further data evaluation, only the coating mass and thickness, as well as the exhaust temperature are viewed at, as all other Q2 values are below 0.5, and therefore the model does not fit these responses well.

For the coating mass, the following statements can be made, visible in Figure 50. At low pattern pressure of 1bar, high flow rates and temperature achieve the highest coating mass. Nevertheless, also low spraying rates and low temperatures show quite good performance. At this pattern pressure, all but small flow rates with high temperature and high flow rates with low temperature show good characteristics. For 1.3bar pattern pressure the temperature and flow rate should be either both high or low for best results. At the highest pattern pressure only small flow rates with a low temperature give good results.
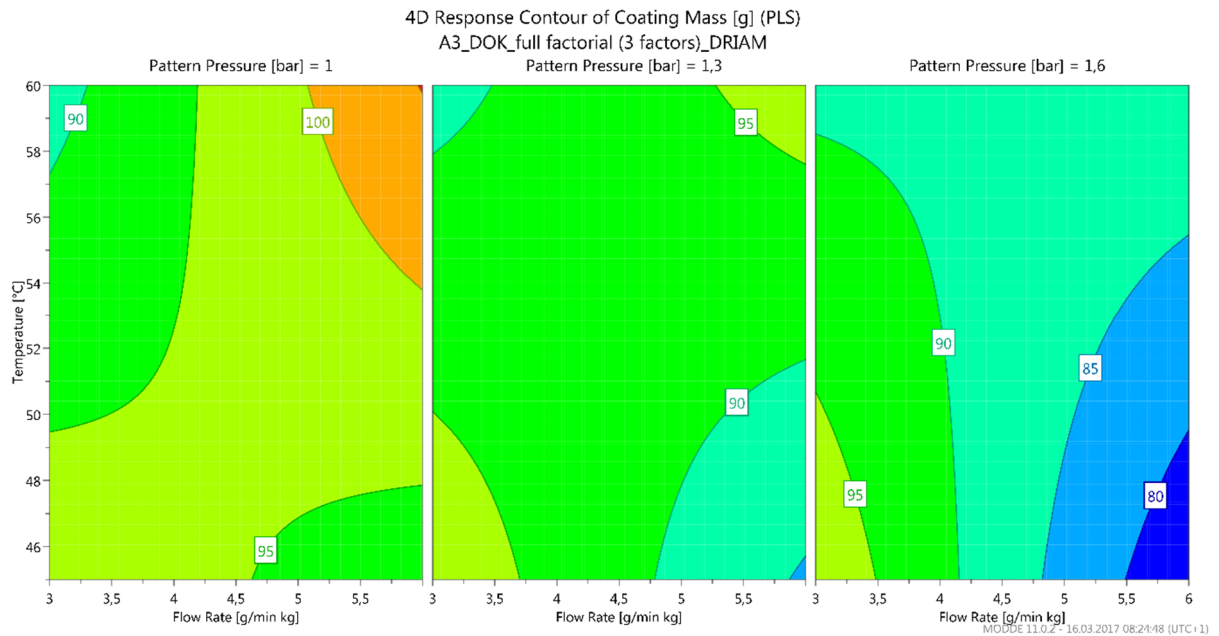
Figure 50: 4D Response Contour Plot of the Coating Mass in MODDE11.

The used coefficients for the modeling of the coating mass are shown in Figure 51. The pattern pressure and flow rate, especially in combination with the temperature and the pattern pressure, show to have the most influence.
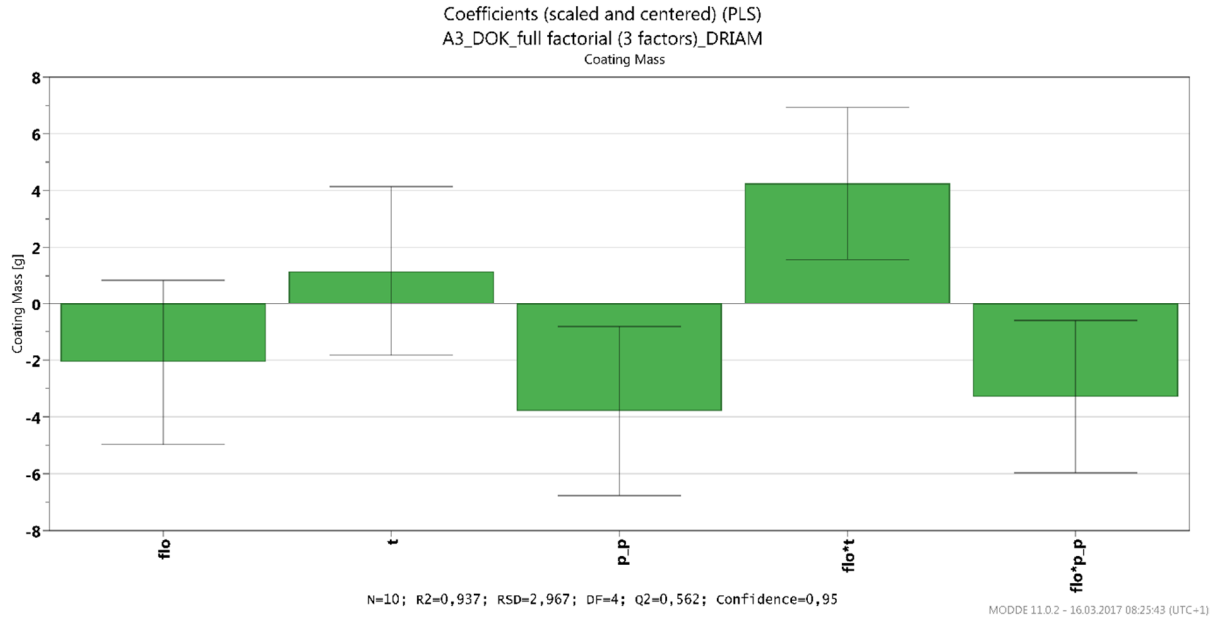
Figure 51: Used coefficients for the modeling of the coating mass.

The coating thickness evaluation, shown in Figure 52, shows very similar characteristics. While good results can be achieved over a broad area at low pattern pressure, but mainly at higher flow rates, the optimal process shifts towards small flow rates and temperature with increasing pressure.
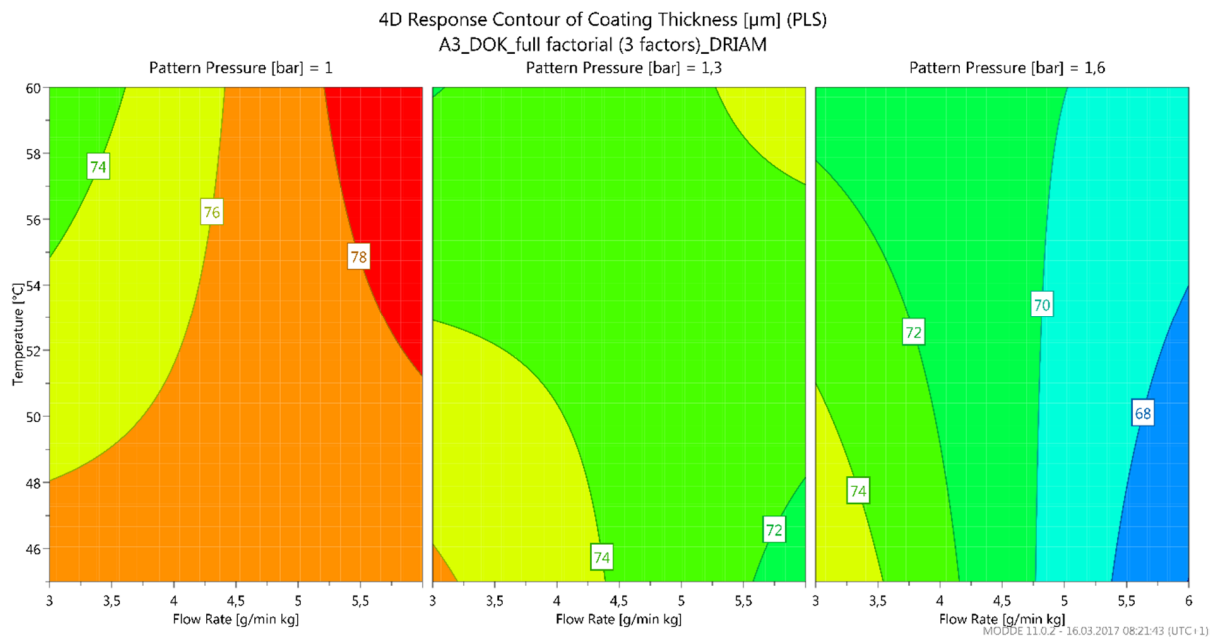
Figure 52: 4D Response Contour Plot of the Coating Thickness in MODDE11.

The coefficients for the coating thickness modelling, visualized in Figure 53, show very similar characteristics, compared to the coating mass coefficients. Again the most influencing parameter is the pattern pressure, but the flow rate influences the outcome especially in combination with the other parameters.
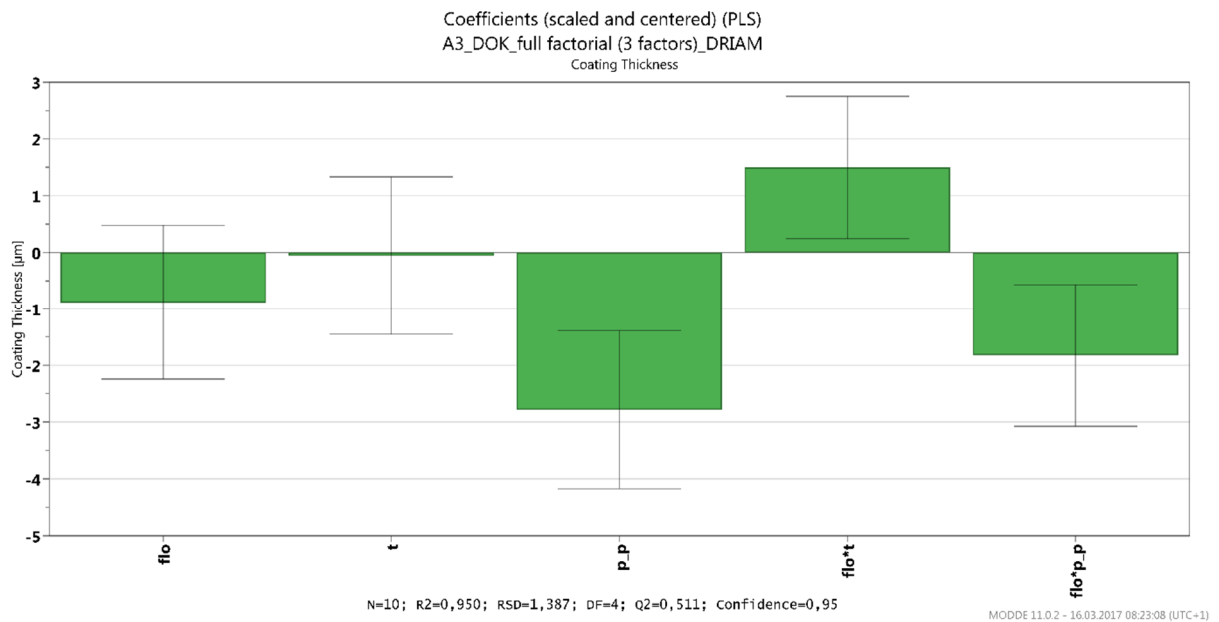
Figure 53 Used coefficients for the modeling of the coating thickness.

The exhaust temperature, shown in Figure 54, shows the following behavior. As the inlet temperature increases, the exhaust temperature increases too. It is interesting however, that

the exhaust temperature increases with the flow rate of the coating suspension, as it would be expected that the necessary solvent evaporation cools the air further down.
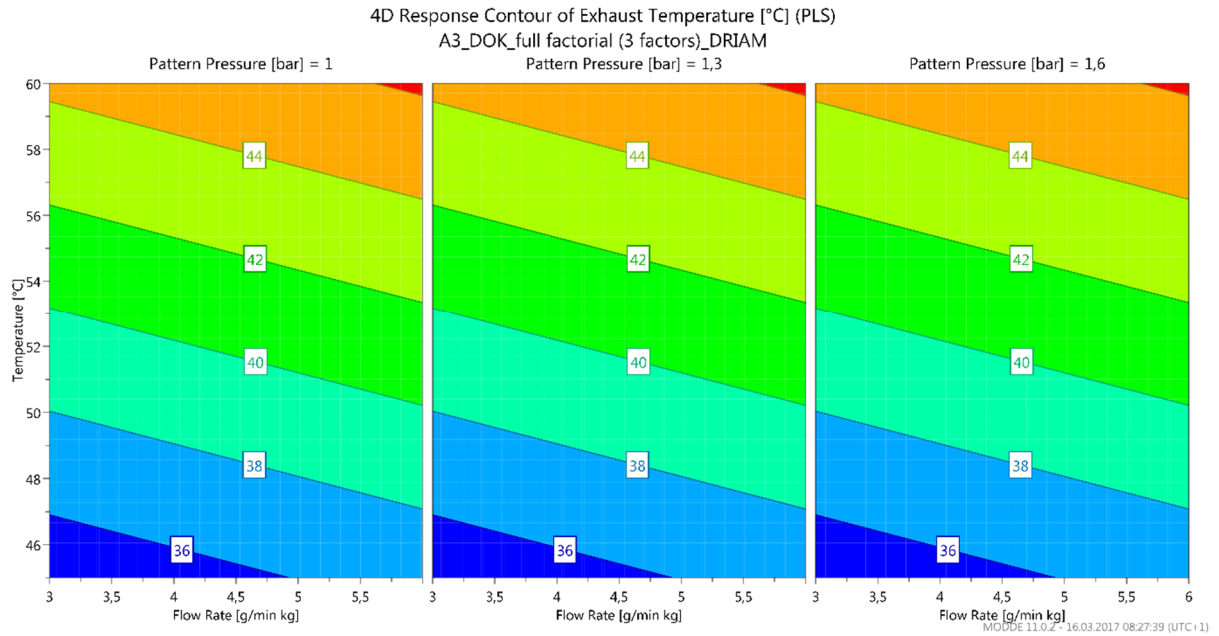
Figure 54: 4D Response Contour Plot of the Exhaust Temperature in MODDE11.

In contrast to the coating mass and thickness modeling, the exhaust temperature is only influenced by the flow rate and the inlet temperature. Visible in Figure 55, the inlet temperature is the most important parameter by a magnitude.
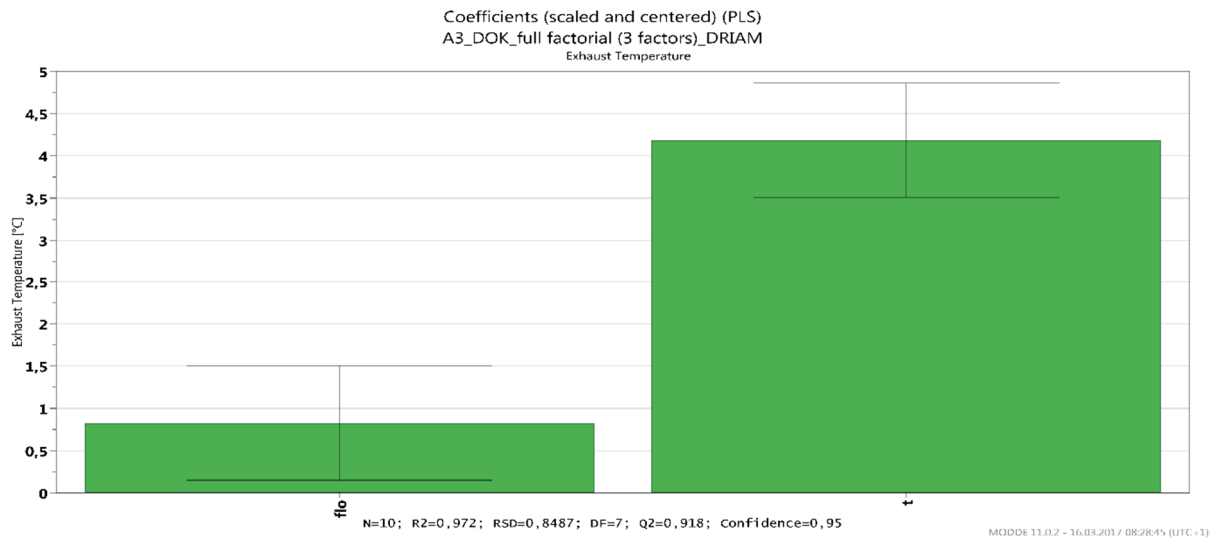
Figure 55: Used coefficients for the modeling of the exhaust temperature.

Based on these three responses, it can be generally said that for maximizing the coating mass and thickness at small pressures, a high flow rate with a high temperature is advised.

4. Conclusion and Outlook

This chapter finalizes and concludes the performed work and the obtained results and connects them to the motivation of this thesis. The scope of this thesis is to investigate the possibility of in-line analysis of coating growth, combined with an analysis of the influence factors on the coating process inside a DRIACONTI-T pharm Lab coater. Also, a mathematical model is created to cross-validate the coating thickness.

The results show that the evaluation of coating thickness inside drum coaters is possible with the means of OCT. An increase of the coating thickness over time is visible, and could be analyzed automatically for future trials. However, there is room for optimization concerning the positioning of the sensor head and the measurement process. Due to the non-sphericity of the drum and the sensor position, only very few tablets are analyzed and the vast majority of pictures contains no information, metal or mirrored tablets. Also, the obtained quality of the coating is improvable, as there is no clear coating layer visible, and therefore the automated evaluation of the in-line data is not possible. This is probably caused by a non-ideal suspension preparation or nozzle problems. This must be avoided for future trials by a better homogenization of the coating suspension and more suitable nozzles, combined with an AC in front of the inlet air to have reproducible processes.

For a profound process understanding, a DoE is created and run at the drum coater. The process is analyzed by measuring the total coating mass, the temperatures of the in- and outgoing airstream and the spray loss. The results of 10 tablets per batch are investigated concerning weight, diameter and coating thickness with its respective standard deviations. The collected data is analyzed in MODDE 11. The analysis shows that the results are generally better when the temperature and flow rate are both high or low, probably linked to the drying capacity of the airstream. The comparison between the mathematical model and the measured coating thickness shows that the obtained results are near, but below the theoretical values. As there is no information for the real density of the film or the coating distribution this correlation needs further investigation.

Concluding, the evaluation of the coating thickness is possible. For further trials or industrial use an ameliorated coating suspension preparation, an improved mounting and adjustment system for the sensor head and optimized nozzles for the used material are advised.

5. References

[1]   FDA, "Guidance for Industry PAT: A Framework for Innovative Pharmaceutical Development, Manufacuring, and Quality Assurance," *FDA Off. Doc.*, no. September, p. 16, 2004.

[2]   M. Kumpugdee-Vollrath, *Easy Coating*, 1st ed. Vieweg+Teubner, 2011.

[3]   C. Cahyadi, A. D. Karande, L. W. Chan, and P. W. S. Heng, "Comparative study of non-destructive methods to quantify thickness of tablet coatings," *Int. J. Pharm.*, vol. 398, no. 1–2, pp. 39–49, 2010.

[4]   M. Zettl, "Implementation of a continuous NIR- Surveillance System for a tableting Process," 2016.

[5]   G. E. Peck, J. L. P. Soh, K. R. Morris, L. L. Augsburger, S. W. Hoag, and H. A. and J. B. S. Leon Lachman, Lieberman, *Pharmaceutical Dosage Forms*, vol. 3. 2008.

[6]   G. E. Peck, J. L. P. Soh, and K. R. Morris, *Dry Granulation*, vol. 1:Unit Ope. 2008.

[7]   S. K. Niazi, *Handbook of Pharmaceutical Manufacturing Formulations - Compressed Solid Products*. Informa Healthcare USA, Inc., 2009.

[8]   World Health Organization, Ed., *The International Pharmacopoeia*, 6th ed. 2016.

[9]   "Pharmaceutical Powder Compaction Technology. Edited by Göran Alderborn and Christer Nyström (Uppsala University). Marcel Dekker, New York, NY. 1996. xv + 610 pp. 15 × 22.5 cm. $185.00. ISBN 0-8247-9376-5.," 1996.

[10]   X. He, "Developing Solid Oral Dosage Forms," *Dev. Solid Oral Dos. Forms*, pp. 407–441, 2009.

[11]   W. Drexler and J. G. Fujimoto, *Optical Coherence Tomohraphy: Technology and Applications*. 2008.

[12]   A. F. Fercher, "Optical coherence tomography - development, principles, applications.," *Z. Med. Phys.*, vol. 20, no. 4, pp. 251–76, Jan. 2010.

[13]   K. A. Serrels, M. K. Renner, and D. T. Reid, "Optical coherence tomography for non-destructive investigation of silicon integrated-circuits," in *Microelectronic Engineering*, 2010, vol. 87, pp. 1785–1791.

References

[14] D. Stifter, K. Wiesauer, M. Wurm, E. Schlotthauer, J. Kastner, M. Pircher, E. Götzinger, and C. K. Hitzenberger, "Investigation of polymer and polymer/fibre composite materials with optical coherence tomography," *Measurement Science and Technology*, vol. 19. p. 74011, 2008.

[15] M. Zettl, "Coating Growth Analysis in a Fluidized Bed with Optical Coherence Tomography," 2014.

[16] D. Markl, M. Zettl, G. Hannesschläger, S. Sacher, M. Leitner, A. Buchsbaum, and J. G. Khinast, "Calibration-free in-line monitoring of pellet coating processes via optical coherence tomography," *Chem. Eng. Sci.*, vol. 125, 2015.

[17] J. A. Zeitler and L. F. Gladden, "In-vitro tomography and non-destructive imaging at depth of pharmaceutical solid dosage forms," *European Journal of Pharmaceutics and Biopharmaceutics*, vol. 71. pp. 2–22, 2009.

[18] S. Zhong, Y. C. Shen, L. Ho, R. K. May, J. A. Zeitler, M. Evans, P. F. Taday, M. Pepper, T. Rades, K. C. Gordon, R. Mller, and P. Kleinebudde, "Non-destructive quantification of pharmaceutical tablet coatings using terahertz pulsed imaging and optical coherence tomography," *Opt. Lasers Eng.*, vol. 49, pp. 361–365, 2011.

[19] D. M. Koller, G. Hannesschläger, M. Leitner, and J. G. Khinast, "Non-destructive analysis of tablet coatings with optical coherence tomography," in *European Journal of Pharmaceutical Sciences*, 2011, vol. 44, pp. 142–148.

[20] T. Fabritius, E. Alarousu, T. Prykäri, J. Hast, and R. Myllylä, "Characterisation of optically cleared paper by optical coherence tomography," *Quantum Electronics*, vol. 36. pp. 181–187, 2007.

[21] J. Czajkowski, T. Prykäri, E. Alarousu, J. Palosaari, R. Myllylä, E. A. Larousu, J. P. Alosaari, R. M. Yllyla, Ã. Ri, and J. C. Zajkowski, "Optical Coherence Tomography as an Accurate Inspection and Quality Evaluation Technique in Paper Industry," *Opt. Rev.*, vol. 17, pp. 218–222, 2010.

[22] M. Wojtkowski, "High-speed optical coherence tomography: basics and applications.," *Appl. Opt.*, vol. 49, no. 16, pp. D30-61, Jun. 2010.

[23] K. Knop and P. Kleinebudde, "PAT-tools for process control in pharmaceutical film coating applications.," *Int. J. Pharm.*, vol. 457, no. 2, pp. 527–36, Dec. 2013.

References

[24]   S. Romero-Torres, J. D. Pérez-Ramos, K. R. Morris, and E. R. Grant, "Raman spectroscopy for tablet coating thickness quantification and coating characterization in the presence of strong fluorescent interference," *J. Pharm. Biomed. Anal.*, vol. 41, no. 3, pp. 811–819, 2006.

[25]   M.-J. Lee, D.-Y. Seo, H.-E. Lee, I.-C. Wang, W.-S. Kim, M.-Y. Jeong, and G. J. Choi, "In line NIR quantification of film thickness on pharmaceutical pellets during a fluid bed coating process.," *Int. J. Pharm.*, vol. 403, no. 1–2, pp. 66–72, Jan. 2011.

[26]   M. Andersson, B. Holmquist, J. Lindquist, O. Nilsson, and K. G. Wahlund, "Analysis of film coating thickness and surface area of pharmaceutical pellets using fluorescence microscopy and image analysis.," *J. Pharm. Biomed. Anal.*, vol. 22, no. 2, pp. 325–39, Mar. 2000.

[27]   "Pamphlet DRIACONTI-T pharma LAB," 2012.

[28]   "Aspirin (Acetyl Salicylic Acid) pharmaceutical secondary standard; traceable to USP, PhEur and BP | Sigma-Aldrich." [Online]. Available: http://www.sigmaaldrich.com/catalog/product/sial/phr1003?lang=de&region=AT. [Accessed: 16-Jan-2017].

[29]   "EUDRAGIT ® L 30 D-55 Specification and Test Methods," 2014.

[30]   "Triethyl citrate 99% | Sigma-Aldrich." [Online]. Available: http://www.sigmaaldrich.com/catalog/product/aldrich/109290?lang=de&region=AT. [Accessed: 15-Jan-2017].

[31]   "Talc tested according to Ph.Eur. | Sigma-Aldrich." [Online]. Available: http://www.sigmaaldrich.com/catalog/product/sial/86257?lang=de&region=AT. [Accessed: 15-Jan-2017].

[32]   "Indigo carmine for microscopy (Bact., Hist.), indicator (pH 11.5-14.0) | Sigma-Aldrich." [Online]. Available: http://www.sigmaaldrich.com/catalog/product/sigma/57000?lang=de&region=AT. [Accessed: 16-Jan-2017].

[33]   "Iron(III) oxide nanopowder,." [Online]. Available: http://www.sigmaaldrich.com/catalog/product/aldrich/544884?lang=de&region=AT. [Accessed: 16-Jan-2017].

References

[34] T. Schmidt-Mende, "Freisetzung aus magensaftresistent überzogenen Arzneiformen."

[35] "Talc: Talc mineral information and data." [Online]. Available: https://www.mindat.org/min-3875.html. [Accessed: 30-Jan-2017].

[36] M. Braun, "Einflussfaktoren bei der Tablettierung magensaftresistent überzogener Pellets auf Exzenter-und Rundlauftablettenpresse," 2003.

[37] K. H. Bauer, *Überzogene Arzneiformen : Grundlagen, Herstellungstechnologien, biopharmazeutische Aspekte, Prüfungsmethoden und Rohstoffe ; mit 45 Tab.* Wiss. Verl.-Ges, 1988.

6. Appendix

6.1. Results of the Offline Measurements

6.1.1. Weight Results

Tablet No	Uncoated Tablets	Exp1	Exp2	Exp3	Exp4	Exp5
[-]	[g]	[g]	[g]	[g]	[g]	[g]
1	0.1995	0.2129	0.2125	0.2183	0.2166	0.2159
2	0.1994	0.2104	0.2149	0.2157	0.2152	0.2169
3	0.1969	0.2154	0.2089	0.2109	0.2156	0.215
4	0.201	0.2136	0.2115	0.2141	0.2138	0.2124
5	0.2074	0.219	0.2145	0.214	0.2184	0.2145
6	0.1996	0.2147	0.2137	0.2157	0.2189	0.2159
7	0.2006	0.2141	0.2142	0.2109	0.2151	0.2107
8	0.2027	0.2172	0.215	0.2112	0.2133	0.2177
9	0.1954	0.2129	0.2177	0.2169	0.2142	0.2138
10	0.2005	0.2171	0.2183	0.2157	0.2167	0.2121
Mean	0.2003	0.21473	0.21412	0.21434	0.21578	0.21449
St.D.	0.00323694	0.00252809	0.00276357	0.00261372	0.0018713	0.00224274

Tablet No	Exp6	Exp7	Exp8	Exp9	Exp10	Exp11
[-]	[g]	[g]	[g]	[g]	[g]	[g]
1	0.2127	0.2141	0.2131	0.2121	0.2107	0.2089
2	0.2128	0.2131	0.2116	0.2102	0.2117	0.2109
3	0.2115	0.2179	0.213	0.2122	0.2123	0.2102
4	0.2153	0.2122	0.2133	0.2132	0.213	0.2142
5	0.2108	0.2144	0.2142	0.2085	0.214	0.2157
6	0.2112	0.2162	0.2153	0.2154	0.2149	0.2157
7	0.2123	0.2181	0.2108	0.2127	0.2084	0.2148
8	0.2139	0.2115	0.2142	0.2153	0.2141	0.215
9	0.2144	0.2137	0.2173	0.2167	0.2137	0.2161
10	0.2148	0.21	0.2091	0.2127	0.2198	0.2139
Mean	0.21297	0.21412	0.21319	0.2129	0.21326	0.21354
St.D.	0.00157201	0.00265154	0.00231922	0.00245855	0.0029908	0.0025782

Appendix

Tablet No	Conti 1	Conti 2	Conti 3	Conti 4
[-]	[g]	[g]	[g]	[g]
1	0.2159	0.2095	0.2102	0.2178
2	0.2139	0.2119	0.2103	0.2131
3	0.215	0.2083	0.2116	0.2147
4	0.2147	0.2086	0.2087	0.2187
5	0.2139	0.2106	0.2124	0.2101
6	0.2144	0.2126	0.2062	0.2121
7	0.2142	0.2149	0.2082	0.2154
8	0.212	0.2116	0.2106	0.2128
9	0.2119	0.2121	0.2107	0.2132
10	0.2145	0.2101	0.2152	0.2091
Mean	0.21404	0.21102	0.21041	0.2137
St.D.	0.00124561	0.00201152	0.00245015	0.00305141

Tablet No	Conti 5	Conti 6	Conti 7
[-]	[g]	[g]	[g]
1	0.2105	0.2122	0.201
2	0.2122	0.2133	0.1966
3	0.2151	0.2115	0.198
4	0.2116	0.2137	0.1973
5	0.2131	0.2098	0.1967
6	0.2127	0.2105	0.1995
7	0.2101	0.2119	0.1986
8	0.2142	0.2099	0.1972
9	0.2138	0.2092	0.1936
10	0.2187	0.2067	0.1995
Mean	0.2132	0.21087	0.1978
St.D.	0.0024931	0.00209605	0.00204396

6.1.2. Diameter Results

Tablet No	Uncoated Tablets	Exp1	Exp2	Exp3	Exp4	Exp5
[-]	[mm]	[mm]	[mm]	[mm]	[mm]	[mm]
1	7.809	7.882	7.889	7.898	7.951	7.975
2	7.811	7.873	7.913	7.914	7.94	7.927
3	7.806	7.879	7.909	7.919	7.951	7.908
4	7.812	7.875	7.902	7.917	7.96	7.923
5	7.821	7.885	7.922	7.904	7.956	7.936
6	7.822	7.889	7.907	7.935	7.955	7.946
7	7.814	7.882	7.905	7.929	7.971	7.921
8	7.824	7.866	7.916	7.943	7.946	7.938
9	7.819	7.871	7.914	7.966	7.956	7.946
10	7.831	7.881	7.935	7.919	7.966	7.925
Mean	7.8169	7.8783	7.9112	7.9244	7.9552	7.9345
St.D.	0.00778103	0.00697695	0.01227282	0.01984495	0.00907744	0.01850676

Tablet No	Exp6	Exp7	Exp8	Exp9	Exp10	Exp11
[-]	[mm]	[mm]	[mm]	[mm]	[mm]	[mm]
1	7.966	7.939	7.924	7.949	7.924	7.916
2	7.961	7.937	7.933	7.955	7.939	7.919
3	7.909	7.929	7.934	7.932	7.942	7.953
4	7.975	7.928	7.946	7.957	7.929	7.971
5	7.929	7.92	8.029	7.959	7.955	7.954
6	7.972	7.925	7.959	7.987	7.922	7.973
7	7.944	7.928	7.956	7.969	7.944	7.96
8	7.953	7.919	7.967	7.963	7.955	7.954
9	7.94	7.939	7.96	7.961	7.938	7.946
10	7.951	7.927	7.943	7.943	7.959	7.938
Mean	7.95	7.9291	7.9551	7.9575	7.9407	7.9484
St.D.	0.0204233	0.00720262	0.02938802	0.01485672	0.01304735	0.01932874

Appendix

Tablet No	Conti 1	Conti 2	Conti 3	Conti 4
[-]	[mm]	[mm]	[mm]	[mm]
1	7.951	7.952	7.965	7.949
2	7.985	7.948	7.944	7.957
3	7.916	7.928	7.91	7.947
4	7.945	7.92	7.919	7.951
5	7.947	7.924	7.912	7.957
6	7.961	7.955	7.904	7.958
7	7.946	7.939	7.87	7.939
8	7.979	7.933	7.892	7.967
9	7.934	7.942	7.915	7.923
10	8.003	7.939	7.939	7.924
Mean	7.9567	7.938	7.917	7.9472
St.D.	0.02584161	0.01177568	0.02708423	0.01456632

Tablet No	Conti 5	Conti 6	Conti 7
[-]	[mm]	[mm]	[mm]
1	7.933	7.927	7.836
2	7.955	7.938	7.863
3	7.953	7.937	7.87
4	7.96	7.942	7.838
5	7.951	7.935	7.851
6	7.965	7.941	7.84
7	7.957	7.938	7.879
8	7.947	7.933	7.845
9	7.963	7.939	7.835
10	7.971	7.946	7.84
Mean	7.9555	7.9376	7.8497
St.D.	0.01061707	0.0052111	0.01563507

6.1.3. 3D-OCT Measurements

6.1.3.1. Exp1

Tablet No	Coating thickness			Mean Coating Thickness	Intra tablet deviation
[#]	[µm]	[µm]	[µm]	[µm]	[µm]
1	75	79.1666667	79.1666667	77.77777778	2.40562612
2	81.25	79.1666667	79.1666667	79.86111111	1.20281306
3	79.1666667	72.9166667	81.25	77.77777778	4.33680417
4	77.0833333	79.1666667	80.2083333	78.81944444	1.59117212
5	79.1666667	75	83.3333333	79.16666667	4.16666667
6	72.9166667	75	76.0416667	74.65277778	1.59117212
7	73.9583333	75	77.0833333	75.34722222	1.59117212
8	79.1666667	78.125	79.1666667	78.81944444	0.60140653
9	75	71.875	77.0833333	74.65277778	2.62147029
10	79.1666667	79.1666667	77.0833333	78.47222222	1.20281306
Mean Coating	77.5347222	1.23971765	1.36391144		
Inter tablet Deviation	1.93705884				
Mean Intra Tablet Deviation	2.13111162				

6.1.3.2. Exp2

Tablet No	Coating thickness			Mean Coating Thickness	Intra tablet Deviation
[#]	[µm]	[µm]	[µm]	[µm]	[µm]
1	87.5	91.6666667	93.75	90.97222222	3.18234423
2	77.0833333	75	79.1666667	77.08333333	2.08333333
3	70.8333333	76.0416667	70.8333333	72.56944444	3.00703265
4	85.4166667	83.3333333	85.4166667	84.72222222	1.20281306
5	72.9166667	68.75	75	72.22222222	3.18234423
6	66.6666667	64.5833333	70.8333333	67.36111111	3.18234423
7	75	72.9166667	76.0416667	74.65277778	1.59117212
8	64.5833333	68.75	70.8333333	68.05555556	3.18234423
9	60.4166667	70.8333333	72.9166667	68.05555556	6.6969797
10	91.6666667	77.0833333	81.25	83.33333333	7.51156516
Mean Coating	75.9027778	5.1546189	2.22862547		
Inter tablet Deviation	8.05409203				
Mean Intra Tablet Deviation	3.48222729				

6.1.3.3. Exp3

Tablet No	Coating thickness			Mean Coating Thickness	Intra tablet Deviation
[#]	[µm]	[µm]	[µm]	[µm]	[µm]
1	77.0833333	70.8333333	76.0416667	74.65277778	3.34848985
2	87.5	89.5833333	95.8333333	90.97222222	4.33680417
3	91.6666667	95.8333333	89.5833333	92.36111111	3.18234423
4	83.3333333	85.4166667	79.1666667	82.63888889	3.18234423
5	77.0833333	81.25	85.4166667	81.25	4.16666667
6	70.8333333	77.0833333	75	74.30555556	3.18234423
7	75	85.4166667	87.5	82.63888889	6.6969797
8	70.8333333	72.9166667	72.9166667	72.22222222	1.20281306
9	79.1666667	81.25	79.1666667	79.86111111	1.20281306
10	81.25	77.0833333	72.9166667	77.08333333	4.16666667
Mean Coating	80.7986111	4.33197193	4.33197193		
Inter tablet Deviation	6.76870614				
Mean Intra Tablet Deviation	3.46682659				

6.1.3.4. Exp4

Tablet No	Coating thickness			Mean Coating Thickness	Intra tablet Deviation
[#]	[µm]	[µm]	[µm]	[µm]	[µm]
1	85.4166667	75	85.4166667	81.94444444	6.0140653
2	75	77.0833333	68.75	73.61111111	4.33680417
3	77.0833333	75	70.8333333	74.30555556	3.18234423
4	79.1666667	87.5	89.5833333	85.41666667	5.5119819
5	79.1666667	83.3333333	89.5833333	84.02777778	5.24294058
6	85.4166667	81.25	84.375	83.68055556	2.16840208
7	79.1666667	83.3333333	83.3333333	81.94444444	2.40562612
8	87.5	85.4166667	83.8541667	85.59027778	1.82910655
9	77.0833333	80.2083333	81.25	79.51388889	2.16840208
10	75	87.5	85.4166667	82.63888889	6.6969797
Mean Coating	81.2673611	2.71784733	2.53162577		
Inter tablet Deviation	4.24663645				
Mean Intra Tablet Deviation	3.95566527				

6.1.3.5. Exp5

Tablet No	Coating thickness			Mean Coating Thickness	Intra tablet Deviation
[#]	[µm]	[µm]	[µm]	[µm]	[µm]
1	75	77.0833333	70.8333333	74.30555556	3.18234423
2	81.25	85.4166667	85.4166667	84.02777778	2.40562612
3	80.2083333	79.1666667	82.2916667	80.55555556	1.59117212
4	72.9166667	77.0833333	76.0416667	75.34722222	2.16840208
5	70.8333333	70.8333333	75	72.22222222	2.40562612
6	79.1666667	70.8333333	76.0416667	75.34722222	4.20984571
7	72.9166667	70.8333333	79.1666667	74.30555556	4.33680417
8	68.75	72.9166667	72.9166667	71.52777778	2.40562612
9	72.9166667	81.25	83.3333333	79.16666667	5.5119819
10	66.6666667	77.0833333	72.9166667	72.22222222	5.24294058
Mean Coating	75.9027778	2.61514005	2.14146363		
Inter tablet Deviation	4.08615633				
Mean Intra Tablet Deviation	3.34603692				

6.1.3.6. Exp6

Tablet No	Coating thickness			Mean Coating Thickness	Intra tablet Deviation
[#]	[µm]	[µm]	[µm]	[µm]	[µm]
1	60.4166667	64.5833333	57.2916667	60.76388889	3.65821311
2	66.6666667	64.5833333	66.6666667	65.97222222	1.20281306
3	66.6666667	68.75	65.625	67.01388889	1.59117212
4	64.5833333	68.75	68.75	67.36111111	2.40562612
5	72.9166667	66.6666667	64.5833333	68.05555556	4.33680417
6	83.3333333	77.0833333	77.0833333	79.16666667	3.60843918
7	62.5	65.625	66.6666667	64.93055556	2.16840208
8	66.6666667	70.8333333	68.75	68.75	2.08333333
9	79.1666667	81.25	78.125	79.51388889	1.59117212
10	50	47.9166667	56.25	51.38888889	4.33680417
Mean Coating	67.2916667	5.20820288	1.72689789		
Inter tablet Deviation	8.137817				
Mean Intra Tablet Deviation	2.69827795				

6.1.3.7. Exp7

Tablet No	Coating thickness			Mean Coating Thickness	Intra tablet Deviation
[#]	[μm]	[μm]	[μm]	[μm]	[μm]
1	79.1666667	70.8333333	65.625	71.875	6.83066513
2	68.75	70.8333333	67.7083333	69.09722222	1.59117212
3	75	70.8333333	67.7083333	71.18055556	3.65821311
4	68.75	72.9166667	75	72.22222222	3.18234423
5	72.9166667	70.8333333	69.7916667	71.18055556	1.59117212
6	75	70.8333333	68.75	71.52777778	3.18234423
7	70.8333333	75	70.8333333	72.22222222	2.40562612
8	68.75	70.8333333	76.0416667	71.875	3.75578258
9	75	77.0833333	71.875	74.65277778	2.62147029
10	72.9166667	71.875	75	73.26388889	1.59117212
Mean Coating	71.9097222	0.92191725	1.94623757		
Inter tablet Deviation	1.4404957				
Mean Intra Tablet Deviation	3.0409962				

6.1.3.8. Exp8

Tablet No	Coating thickness			Mean Coating Thickness	Intra tablet Deviation
[#]	[μm]	[μm]	[μm]	[μm]	[μm]
1	60.4166667	64.5833333	64.5833333	63.19444444	2.40562612
2	62.5	68.75	66.6666667	65.97222222	3.18234423
3	60.4166667	62.5	62.5	61.80555556	1.20281306
4	77.0833333	71.875	75	74.65277778	2.62147029
5	66.6666667	75	68.75	70.13888889	4.33680417
6	70.8333333	70.8333333	68.75	70.13888889	1.20281306
7	62.5	66.6666667	60.4166667	63.19444444	3.18234423
8	70.8333333	79.1666667	77.0833333	75.69444444	4.33680417
9	66.6666667	66.6666667	70.8333333	68.05555556	2.40562612
10	72.9166667	79.1666667	70.8333333	74.30555556	4.33680417
Mean Coating	68.7152778	3.27680463	1.86966078		
Inter tablet Deviation	5.12000723				
Mean Intra Tablet Deviation	2.92134496				

6.1.3.9. Exp9

Tablet No	Coating thickness			Mean Coating Thickness	Intra tablet Deviation
[#]	[µm]	[µm]	[µm]	[µm]	[µm]
1	66.6666667	72.9166667	77.0833333	72.22222222	5.24294058
2	70.8333333	72.9166667	72.9166667	72.22222222	1.20281306
3	71.875	75	73.9583333	73.61111111	1.59117212
4	79.1666667	72.9166667	75	75.69444444	3.18234423
5	77.0833333	83.3333333	81.25	80.55555556	3.18234423
6	68.75	75	72.9166667	72.22222222	3.18234423
7	62.5	75	70.8333333	69.44444444	6.36468847
8	70.8333333	68.75	70.8333333	70.13888889	1.20281306
9	70.8333333	70.8333333	72.9166667	71.52777778	1.20281306
10	70.8333333	62.5	66.6666667	66.66666667	4.16666667
Mean Coating	72.4305556	2.39844486	1.95334014		
Inter tablet Deviation	3.74757009				
Mean Intra Tablet Deviation	3.05209397				

6.1.3.10. Exp10

Tablet No	Coating thickness			Mean Coating Thickness	Intra tablet Deviation
[#]	[µm]	[µm]	[µm]	[µm]	[µm]
1	64.5833333	70.8333333	68.75	68.05555556	3.18234423
2	75	77.0833333	71.875	74.65277778	2.62147029
3	70.8333333	79.1666667	77.0833333	75.69444444	4.33680417
4	68.75	70.8333333	75	71.52777778	3.18234423
5	77.0833333	75	77.0833333	76.38888889	1.20281306
6	72.9166667	75	75	74.30555556	1.20281306
7	75	77.0833333	75	75.69444444	1.20281306
8	68.75	70.8333333	70.8333333	70.13888889	1.20281306
9	79.1666667	77.0833333	79.1666667	78.47222222	1.20281306
10	64.5833333	66.6666667	70.8333333	67.36111111	3.18234423
Mean Coating	73.2291667	2.39901672	1.44123984		
Inter tablet Deviation	3.74846362				
Mean Intra Tablet Deviation	2.25193725				

Appendix

6.1.3.11. Exp11

Tablet No	Coating thickness			Mean Coating Thickness	Intra tablet Deviation
[#]	[µm]	[µm]	[µm]	[µm]	[µm]
1	78.125	75	79.1666667	77.43055556	2.16840208
2	72.9166667	70.8333333	75	72.91666667	2.08333333
3	62.5	64.5833333	65.625	64.23611111	1.59117212
4	77.0833333	79.1666667	77.0833333	77.77777778	1.20281306
5	77.0833333	70.8333333	75	74.30555556	3.18234423
6	70.8333333	70.8333333	68.75	70.13888889	1.20281306
7	70.8333333	68.75	73.9583333	71.18055556	2.62147029
8	77.0833333	77.0833333	70.8333333	75	3.60843918
9	70.8333333	72.9166667	70.8333333	71.52777778	1.20281306
10	70.8333333	70.8333333	66.6666667	69.44444444	2.40562612
Mean Coating	72.3958333	2.59206344	1.3612305		
Inter tablet Deviation	4.05009912				
Mean Intra Tablet Deviation	2.12692265				

6.1.3.12. Conti1

Tablet No	Coating thickness			Mean Coating Thickness	Intra tablet Deviation
[#]	[µm]	[µm]	[µm]	[µm]	[µm]
1	66.6666667	64.5833333	68.75	66.66666667	2.08333333
2	66.6666667	66.6666667	68.75	67.36111111	1.20281306
3	66.6666667	70.8333333	70.8333333	69.44444444	2.40562612
4	75	68.75	72.9166667	72.22222222	3.18234423
5	70.8333333	72.9166667	72.9166667	72.22222222	1.20281306
6	62.5	60.4166667	64.5833333	62.5	2.08333333
7	72.9166667	77.0833333	76.0416667	75.34722222	2.16840208
8	77.0833333	75	78.125	76.73611111	1.59117212
9	77.0833333	81.25	85.4166667	81.25	4.16666667
10	72.9166667	75	76.0416667	74.65277778	1.59117212
Mean Coating	71.8402778	3.52369989	1.38737127		
Inter tablet Deviation	5.50578108				
Mean Intra Tablet Deviation	2.16776761				

6.1.3.13. Conti2

Tablet No	Coating thickness			Mean Coating Thickness	Intra tablet Deviation
[#]	[µm]	[µm]	[µm]	[µm]	[µm]
1	68.75	64.5833333	64.5833333	65.97222222	2.40562612
2	68.75	68.75	62.5	66.66666667	3.60843918
3	64.5833333	66.6666667	66.6666667	65.97222222	1.20281306
4	56.25	58.3333333	61.4583333	58.68055556	2.62147029
5	62.5	64.5833333	64.5833333	63.88888889	1.20281306
6	64.5833333	64.5833333	70.8333333	66.66666667	3.60843918
7	62.5	66.6666667	66.6666667	65.27777778	2.40562612
8	66.6666667	77.0833333	72.9166667	72.22222222	5.24294058
9	62.5	68.75	64.5833333	65.27777778	3.18234423
10	62.5	70.8333333	68.75	67.36111111	4.33680417
Mean Coating	65.7986111	2.13469607	1.90830822		
Inter tablet Deviation	3.3354626				
Mean Intra Tablet Deviation	2.9817316				

6.1.3.14. Conti3

Tablet No	Coating thickness			Mean Coating Thickness	Intra tablet Deviation
[#]	[µm]	[µm]	[µm]	[µm]	[µm]
1	68.75	68.75	62.5	66.66666667	3.60843918
2	37.5	43.75	43.75	41.66666667	3.60843918
3	66.6666667	68.75	56.25	63.88888889	6.6969797
4	64.5833333	60.4166667	66.6666667	63.88888889	3.18234423
5	60.4166667	58.3333333	52.0833333	56.94444444	4.33680417
6	41.6666667	39.5833333	41.6666667	40.97222222	1.20281306
7	62.5	52.0833333	58.3333333	57.63888889	5.24294058
8	72.9166667	77.0833333	64.5833333	71.52777778	6.36468847
9	39.5833333	39.5833333	43.75	40.97222222	2.40562612
10	62.5	56.25	56.25	58.33333333	3.60843918
Mean Coating	56.25	7.21832753	2.57648089		
Inter tablet Deviation	11.2786368				
Mean Intra Tablet Deviation	4.02575139				

6.1.3.15. Conti4

Tablet No	Coating thickness			Mean Coating Thickness	Intra tablet Deviation
[#]	[µm]	[µm]	[µm]	[µm]	[µm]
1	70.8333333	64.5833333	66.6666667	67.36111111	3.18234423
2	54.1666667	50	56.25	53.47222222	3.18234423
3	75	70.8333333	60.4166667	68.75	7.51156516
4	64.5833333	70.8333333	68.75	68.05555556	3.18234423
5	27.0833333	31.25	22.9166667	27.08333333	4.16666667
6	68.75	66.6666667	60.4166667	65.27777778	4.33680417
7	68.75	66.6666667	70.8333333	68.75	2.08333333
8	66.6666667	66.6666667	60.4166667	64.58333333	3.60843918
9	58.3333333	64.5833333	58.3333333	60.41666667	3.60843918
10	66.6666667	77.0833333	72.9166667	72.22222222	5.24294058
Mean Coating	61.5972222	8.45626204	2.56673414		
Inter tablet Deviation	13.2129094				
Mean Intra Tablet Deviation	4.0105221				

6.1.3.16. Conti5

Tablet No	Coating thickness			Mean Coating Thickness	Intra tablet Deviation
[#]	[µm]	[µm]	[µm]	[µm]	[µm]
1	72.9166667	70.8333333	79.1666667	74.30555556	4.33680417
2	70.8333333	72.9166667	68.75	70.83333333	2.08333333
3	62.5	60.4166667	59.375	60.76388889	1.59117212
4	66.6666667	64.5833333	72.9166667	68.05555556	4.33680417
5	68.75	66.6666667	68.75	68.05555556	1.20281306
6	62.5	68.75	64.5833333	65.27777778	3.18234423
7	66.6666667	75	68.75	70.13888889	4.33680417
8	68.75	66.6666667	69.7916667	68.40277778	1.59117212
9	72.9166667	79.1666667	64.5833333	72.22222222	7.31642622
10	68.75	68.75	75	70.83333333	3.60843918
Mean Coating	68.8888889	2.43477324	2.14951122		
Inter tablet Deviation	3.80433318				
Mean Intra Tablet Deviation	3.35861128				

6.1.3.17. Conti6

Tablet No	Coating thickness			Mean Coating Thickness	Intra tablet Deviation
[#]	[µm]	[µm]	[µm]	[µm]	[µm]
1	72.9166667	68.75	66.6666667	69.44444444	3.18234423
2	66.6666667	70.8333333	62.5	66.66666667	4.16666667
3	54.1666667	68.75	70.8333333	64.58333333	9.08103947
4	68.75	64.5833333	62.5	65.27777778	3.18234423
5	58.3333333	56.25	56.25	56.94444444	1.20281306
6	54.1666667	56.25	54.1666667	54.86111111	1.20281306
7	58.3333333	62.5	65.625	62.15277778	3.65821311
8	60.4166667	68.75	56.25	61.80555556	6.36468847
9	56.25	60.4166667	62.5	59.72222222	3.18234423
10	56.25	54.1666667	64.5833333	58.33333333	5.5119819
Mean Coating	61.9791667	2.93925702	2.6070559		
Inter tablet Deviation	4.59258909				
Mean Intra Tablet Deviation	4.07352484				

6.1.3.18. Conti7

Tablet No	Coating thickness			Mean Coating Thickness	Intra tablet Deviation
[#]	[µm]	[µm]	[µm]	[µm]	[µm]
1	20.8333333	14.5833333	16.6666667	17.36111111	3.18234423
2	14.5833333	20.8333333	10.4166667	15.27777778	5.24294058
3	14.5833333	14.5833333	16.6666667	15.27777778	1.20281306
4	14.5833333	10.4166667	10.4166667	11.80555556	2.40562612
5	12.5	9.375	8.33333333	10.06944444	2.16840208
6	7.29166667	7.29166667	8.33333333	7.638888889	0.60140653
7	10.4166667	8.33333333	10.4166667	9.722222222	1.20281306
8	12.5	10.4166667	14.5833333	12.5	2.08333333
9	10.4166667	14.5833333	8.33333333	11.11111111	3.18234423
10	10.4166667	10.4166667	8.33333333	9.722222222	1.20281306
Mean Coating	12.0486111	1.95995577	1.43838952		
Inter tablet Deviation	3.06243089				
Mean Intra Tablet Deviation	2.24748363				

6.1.4. DRIAM Parameters and Temperature

6.1.4.1. Exp1

RPM	22	[rpm]
T_inlet	45	[°C]
Air Fan	50	[%]
m_tablets	1400	[g]
p_atom	0.7	[bar]
p_pattern	1	[bar]
g_min_kg	3	[g/min/kg]
g_min	4.2	[g/min]
pump_power	9.25	[%]
Coating_sprayed	680	[g]
Coating_mass	99.5	[g]
t_coat	167	[min]
g_min_actual	4.07185629	[g/min]
spray loss	0.26838235	

t	T_inlet	T_1	T_2	T_3
[hh:mm]	[°C]	[°C]	[°C]	[°C]
15:50	46.8	42.1	41.4	40.7
15:55	45.1	41.6	40.5	37.9
16:00	45	41	39.5	36.3
16:05	45	40.9	38.8	35.5
16:10	45	40.4	38	35.1
16:15	44.9	40	37.8	34.9
16:20	45	40.2	38	34.1
16:25	44.9	40.1	38	34
16:30	44.6	40.1	38	34
16:40	45.2	40.1	37.9	33.6
16:45	45	40.1	37.8	33.8
17:00	45	40	37.9	33.8
17:15	44.8	40.1	37.9	34
17:30	45	40.1	37.9	33.8
17:45	44.8	40.1	37.9	34.3
18:00	45	40	37.8	34.5
18:15	45	39.8	37.6	34.8
18:30	45	40	38.2	34.6
18:37	45	40	38.1	35.1

6.1.4.2. Exp2

RPM	22	[rpm]
T_inlet	45	[°C]
Air Fan	50	[%]
m_tablets	1400	[g]
p_atom	0.7	[bar]
p_pattern	1	[bar]
g_min_kg	6	[g/min/kg]
g_min	8.4	[g/min]
pump_power	19.99	[%]
Coating_sprayed	780	[g]
Coating_mass	93	[g]
t_coat	84	[min]
g_min_actual	9.28571429	[g/min]
spray loss	0.40384615	

t	T_inlet	T_1	T_2	T_3
[hh:mm]	[°C]	[°C]	[°C]	[°C]
11:45	45.2	43.6	43.1	43.6
11:50	45	43.2	41.7	37.1
11:55	45.1	43	41.2	35.8
12:00	45	43	41	35.8
12:05	45	43.2	41.2	35.1
12:10	45	43.1	41.3	34.8
12:15	45.1	43	41.3	35.8
12:20	45	43	41.1	35.7
12:25	46.1	43.4	41.5	36.6
12:30	45.1	43.2	41.2	36.2
12:45	45	43	41.1	35.5
13:00	45	43	40.9	36.3
13:09	45.1	43	40.9	37.1

6.1.4.3. Exp3

RPM	22	[rpm]
T_inlet	60	[°C]
Air Fan	50	[%]
m_tablets	1400	[g]
p_atom	0.7	[bar]
p_pattern	1	[bar]
g_min_kg	3	[g/min/kg]
g_min	4.2	[g/min]
pump_power	10.5	[%]
Coating_sprayed	675.2	[g]
Coating_mass	82.4	[g]
t_coat	167	[min]
g_min_actual	4.04311377	[g/min]
spray loss	0.38981043	

t	T_inlet	T_1	T_2	T_3
[hh:mm]	[°C]	[°C]	[°C]	[°C]
10:53	59.8	55	54.1	53.7
10:55	60.1	54.3	53	51.8
11:00	61.7	53	50.9	48.6
11:05	59.1	51.5	49.3	47.8
11:10	60.1	51.3	49.4	47.3
11:15	59.9	51.2	49.5	47
11:20	60	51.2	49.3	47.2
11:25	60.1	51.2	49.2	47.5
11:40	59.9	51.4	49.6	47.1
11:55	62	51.3	49	46.1
12:10	59	50.8	48.6	45.5
12:25	60	51	49	46.6
12:40	59.3	51	48.6	46.3
12:55	59.9	50.5	48.1	45.9
13:10	60	50.7	48.1	45
13:25	61.7	50.9	48.3	45.3
13:40	60	50.4	48	45.3

6.1.4.4. Exp4

RPM	22	[rpm]
T_inlet	60	[°C]
Air Fan	50	[%]
m_tablets	1400	[g]
p_atom	0.7	[bar]
p_pattern	1	[bar]
g_min_kg	6	[g/min/kg]
g_min	8.4	[g/min]
pump_power	19.51	[%]
Coating_sprayed	710	[g]
Coating_mass	106.8	[g]
t_coat	84	[min]
g_min_actual	8.45238095	[g/min]
spray loss	0.24788732	

t	T_inlet	T_1	T_2	T_3
[hh:mm]	[°C]	[°C]	[°C]	[°C]
08:05	60	54.3	53.6	52.6
08:10	59.9	52.8	51.1	47
08:15	59.9	52.1	49.8	45.1
08:20	59.9	51.8	49.3	44.7
08:25	59.8	52.1	49.8	45.1
08:30	59.9	52.1	49.6	44.5
08:35	59.9	52.2	49.5	45
08:40	60.1	52.3	49.7	45.1
08:45	60	52.3	49.8	45.8
08:50	60	52.4	49.9	45.5
08:55	60	52.5	50.3	45.3
09:00	60	52.5	50.1	45.4
09:05	60.1	52.6	50	46
09:10	59.9	52.6	50.1	45.9
09:15	60	52.6	50.2	45.5
09:20	60	52.7	50.1	46
09:25	60	52.5	50.1	45.9
09:29	60	52.6	50.2	45.8

6.1.4.5. Exp5

RPM	22	[rpm]
T_inlet	45	[°C]
Air Fan	50	[%]
m_tablets	1400	[g]
p_atom	0.7	[bar]
p_pattern	1.6	[bar]
g_min_kg	3	[g/min/kg]
g_min	4.2	[g/min]
pump_power	8.75	[%]
Coating_sprayed	618	[g]
Coating_mass	99.2	[g]
t_coat	167	[min]
g_min_actual	3.7005988	[g/min]
spray loss	0.197411	

t	T_inlet	T_1	T_2	T_3
[hh:mm]	[°C]	[°C]	[°C]	[°C]
14:50	45.4	42.9	42.1	40.6
14:55	45	42.1	39.9	37
15:00	46.9	41.7	39.1	35.8
15:05	44.8	40.5	38	34.8
15:10	44.9	40.3	37.9	34.7
15:15	45.1	40.2	37.8	34.6
15:20	45.1	40.4	37.7	34.3
15:25	44.5	40.1	37.5	34
15:30	44.8	39.9	37.2	34
15:45	45.5	39.8	37.1	33.6
16:00	44.8	39.5	36.9	33.3
16:15	44.6	39.3	36.8	33.5
16:30	45	39.1	36.8	33.3
16:45	47.1	39.4	37.1	34.1
17:00	44	39.1	36.6	33.3
17:15	46.3	41.3	40.2	36.2
17:30	46.4	39.6	36.9	35.6
17:37	45.3	38.7	36.7	34.9

6.1.4.6. Exp6

RPM	22	[rpm]
T_inlet	45	[°C]
Air Fan	50	[%]
m_tablets	1400	[g]
p_atom	0.7	[bar]
p_pattern	1.6	[bar]
g_min_kg	6	[g/min/kg]
g_min	8.4	[g/min]
pump_power	19.99	[%]
Coating_sprayed	642	[g]
Coating_mass	78	[g]
t_coat	84	[min]
g_min_actual	7.64285714	[g/min]
spray loss	0.39252336	

t	T_inlet	T_1	T_2	T_3
[hh:mm]	[°C]	[°C]	[°C]	[°C]
15:17	45.1	45.5	44.6	44.1
15:20	45.1	45.2	43.8	41.1
15:25	45.1	44.4	42.4	37.8
15:30	45	43.8	41.7	36.8
15:35	45	43.6	41.3	36.2
15:40	45	43.2	41	35.9
15:45	45	43	40.6	35.9
16:00	45	42.8	40.6	34.8
16:15	45	42.6	40.3	35.8
16:30	44.8	42.5	40.1	35.6
16:41	45	42.5	40.1	35.4

6.1.4.7. Exp7

RPM	22	[rpm]
T_inlet	60	[°C]
Air Fan	50	[%]
m_tablets	1400	[g]
p_atom	0.7	[bar]
p_pattern	1.6	[bar]
g_min_kg	3	[g/min/kg]
g_min	4.2	[g/min]
pump_power	8.75	[%]
Coating_sprayed	669.2	[g]
Coating_mass	90.4	[g]
t_coat	167	[min]
g_min_actual	4.00718563	[g/min]
spray loss	0.32456665	

t	T_inlet	T_1	T_2	T_3
[hh:mm]	[°C]	[°C]	[°C]	[°C]
11:15	61.6	55.4	54.4	54.9
11:20	59.9	53.9	52.1	50.4
11:25	62	52.4	49.8	47.5
11:30	61.4	51.9	48.9	45.8
11:35	59.9	51.1	48	44.4
11:40	59.6	50.6	47.5	44.1
11:45	59.8	50.5	47.6	44.1
12:00	60.1	50.6	47.9	45
12:15	59.8	50.6	48.1	45.1
12:30	60.1	50.7	47.5	43.8
12:45	60	50.8	47.8	44
13:00	59.6	50.4	47.1	43.2
13:15	58.6	50.1	47.1	43.4
13:30	59.3	50.5	47.2	43.5
13:45	60.3	50.5	47.3	43.5
13:58	60	50.4	47.2	43.5

6.1.4.8. Exp8

RPM	22	[rpm]
T_inlet	60	[°C]
Air Fan	50	[%]
m_tablets	1400	[g]
p_atom	0.7	[bar]
p_pattern	1.6	[bar]
g_min_kg	6	[g/min/kg]
g_min	8.4	[g/min]
pump_power	19.99	[%]
Coating_sprayed	753	[g]
Coating_mass	89.3	[g]
t_coat	84	[min]
g_min_actual	8.96428571	[g/min]
spray loss	0.40703851	

t	T_inlet	T_1	T_2	T_3
[hh:mm]	[°C]	[°C]	[°C]	[°C]
13:30	60.2	52	51.2	49.8
13:35	60.3	52.6	51	46.1
13:40	60	53.4	51.2	45.6
13:45	60	53.6	51.3	46.1
13:50	60.1	54	51.5	46.5
13:55	60.1	54.1	51.8	46.1
14:00	60	54.3	51.9	46.3
14:15	60.1	54.1	51.5	46.4
14:30	60.1	54.6	52.2	46.3
14:45	60	54.6	52.1	47.1
14:54	59.9	54.8	52.5	47

6.1.4.9. Exp9

RPM	22	[rpm]
T_inlet	52.5	[°C]
Air Fan	60	[%]
m_tablets	1400	[g]
p_atom	0.7	[bar]
p_pattern	1.3	[bar]
g_min_kg	4.5	[g/min/kg]
g_min	6.3	[g/min]
pump_power	16.2	[%]
Coating_sprayed	727.4	[g]
Coating_mass	88.4	[g]
t_coat	112	[min]
g_min_actual	6.49464286	[g/min]
spray loss	0.39235634	

t	T_inlet	T_1	T_2	T_3
[hh:mm]	[°C]	[°C]	[°C]	[°C]
08:10	53.1	48.5	47.5	48
08:15	52.4	47.1	45.5	43.6
08:20	52.5	46.6	44.8	42.3
08:25	52.5	45.9	43.4	40.8
08:30	52.3	45.6	43	40.8
08:35	52.4	45.5	42.6	40.3
08:40	53	45.3	42.6	40.1
08:45	52.3	45.2	42.6	39.6
08:50	52.5	45.3	42.8	39.5
08:55	52.5	45.3	42.6	39.8
09:00	54	45.9	43.3	40.1
09:05	52.6	45.6	43.1	39.5
09:10	52.1	45.5	42.9	39.2
09:15	52.3	45.5	43	39.4
09:20	52.5	46	44.1	41.7
09:25	52.5	45.8	43.8	41
09:30	52.5	46	44	41
09:45	52.4	45.8	43.6	40.8
10:00	52.2	45.7	43.6	41.1
10:02	52.5	45.7	43.8	41

6.1.4.10. Exp10

RPM	22	[rpm]
T_inlet	52.5	[°C]
Air Fan	50	[%]
m_tablets	1400	[g]
p_atom	0.7	[bar]
p_pattern	1.3	[bar]
g_min_kg	4.5	[g/min/kg]
g_min	6.3	[g/min]
pump_power	17.8	[%]
Coating_sprayed	637.1	[g]
Coating_mass	89	[g]
t_coat	112	[min]
g_min_actual	5.68839286	[g/min]
spray loss	0.30152252	

t	T_inlet	T_1	T_2	T_3
[hh:mm]	[°C]	[°C]	[°C]	[°C]
14:10	54.2	51.4	51	50.3
14:15	52.3	48.7	46.8	43.4
14:25	52.4	47.3	44.8	40.6
14:30	53.1	46.8	44	39.7
14:35	52.3	46.3	43.5	39.1
14:40	52.6	46.1	43.3	39
14:45	52.3	45.9	43.1	39.2
15:00	52.2	45.6	43	39.3
15:15	52.3	45.5	42.7	39.6
15:30	53.4	45.9	43.5	38.9
15:45	52.5	45.9	43.5	39.8
16:00	52.5	47.8	47	47.3

6.1.4.11. Exp11

RPM	22	[rpm]
T_inlet	52.5	[°C]
Air Fan	50	[%]
m_tablets	1400	[g]
p_atom	0.7	[bar]
p_pattern	1.3	[bar]
g_min_kg	4.5	[g/min/kg]
g_min	6.3	[g/min]
pump_power	14.98	[%]
Coating_sprayed	681	[g]
Coating_mass	91	[g]
t_coat	112	[min]
g_min_actual	6.08035714	[g/min]
spray loss	0.3318649	

t	T_inlet	T_1	T_2	T_3
[hh:mm]	[°C]	[°C]	[°C]	[°C]
17:10	53.2	49.5	48.6	48.2
17:15	52.5	49.1	47.6	44.1
17:20	52.5	49.1	47.1	42.4
17:25	52.4	49	47	42
17:30	52.5	49	47	41.5
17:35	52.4	48.9	46.8	41.6
17:40	52.5	48.9	47	41.6
17:45	52.6	49	47	41.3
18:00	52.6	48.9	46.9	42.5
18:15	52.6	49	46.7	43.3
18:30	52.6	49	46.9	41.3
18:45	52.4	49.2	47.5	44
19:02	52.4	49	47	41.6

6.1.4.12. Continuous Run

RPM	22	[rpm]
T_inlet	52.5	[°C]
Air Fan	50	[%]
m_tablets	1400	[g]
p_atom	0.7	[bar]
p_pattern	1.3	[bar]
g_min_kg	4.5	[g/min/kg]
g_min	6.3	[g/min]
pump_power_1	7.43	[%]
pump_power_2	14.5	[%]
Pump_power_3	15.5	[%]
t_coat	112	[min]
g_coating_1	74.5	[g]
g_coating_2	94	[g]
g_coating_3	100.5	[g]
g_coating_4	78.3	[g]
g_coating_5	78.7	[g]
g_coating_6	75.5	[g]
g_coating_7	8.4	[g]
coating_sprayed	3588	[g]

t	T_inlet	T_1	T_2	T_3
[hh:mm]	[°C]	[°C]	[°C]	[°C]
11:50	52.8	44.9	47.1	47.9
11:55	52.6	41.8	45.7	46.4
12:00	52.5	41.4	45.6	46.5
12:05	52.6	41.5	45.1	46.1
12:10	52.5	41.8	45.8	46.7
12:15	52.6	42	45.7	46.6
12:20	52.5	42.3	46.1	47
12:25	52.5	43.1	46.3	47.1
12:30	52.5	41.1	41.4	47
12:35	52.5	41.9	39.1	46.5
12:40	52.4	41.6	39.1	46.5
12:45	52.5	42	38.9	46.5
12:50	52.5	41.6	38.8	46.5
12:55	52.4	42.1	38.9	46.5
13:00	52.6	41.2	39.3	46.6
13:05	52.8	41.6	41.1	43.5
13:10	52.5	42.9	39.3	42
13:15	52.5	42.6	38.8	41.6
13:20	52.5	43.1	39.3	41.9
13:25	52.5	43.1	39	41.8
13:30	52.4	42.6	38.7	41.5

13:35	52.5	42.1	38.6	40.5
13:40	52.5	43.1	38.8	41.8
13:45	52.5	42.5	40.4	42.9
13:50	52.4	43	39.4	42.3
13:55	52.5	42.8	39.2	42.5
14:00	52.6	42.7	39.5	42.8
14:05	52.4	42.8	38.9	42
14:10	52.5	43.4	39.1	42.1
14:15	52.4	42.6	39	42.3
14:20	52.6	43.7	40.8	43.5
14:25	52.6	43.3	40	42.9
14:30	52.6	43.5	39.8	42.5
14:35	52.5	43.6	39.6	42.3
14:40	52.4	43	39.7	42.4
14:45	52.4	43.4	39.4	43.1
14:50	52.4	42.9	39.8	42.3
14:55	52.6	43	39.5	42.1
15:00	52.5	43.3	40.3	43
15:05	52.6	43.2	39.8	43.4
15:10	52.6	42.7	39.6	42.8
15:15	52.4	42.4	39.3	42
15:20	52.4	42.2	39.1	41.7
15:25	52.6	43.1	39.5	43.9
15:30	52.5	43.2	39.4	42.5
15:35	52.8	42.9	40.8	42.9
15:40	52.2	45.1	40.2	42.1
15:45	53.1	48	44.6	45.7
15:50	52.5	47.5	41	42.9
15:55	52.5	47.5	41	42.8
16:00	52.5	47.5	41.1	42.7
16:05	52.5	47.1	40.6	42
16:10	52.5	47.8	46.2	44
16:15	52.6	48.5	46.8	43
16:20	52.5	48.6	47	42.9
16:25	52.6	48.5	47	43.3
16:30	52.6	48.5	47	43.3
16:35	52.5	48.6	47.1	43.6
16:40	52.4	48.8	47.1	43.3